Virchows Arch (2005) 447: 53–60
DOI 10.1007/s00428-005-1275-6

ORIGINAL ARTICLE

Naoya Nakamura · Hidenori Hase · Daisuke Sakurai · Sachiko Yoshida · Masafumi Abe · Nobuhiro Tsukada · Jun Takizawa · Sadao Aoki · Masaru Kojima · Shigeo Nakamura · Tetsuji Kobata

Expression of BAFF-R (BR3) in normal and neoplastic lymphoid tissues characterized with a newly developed monoclonal antibody

Received: 10 January 2005 / Accepted: 12 April 2005 / Published online: 14 June 2005

Abstract BAFF-receptor (BAFF-R) is required for the successful maturation and survival of B-cells. We developed an anti-human BAFF-R monoclonal antibody (mAb), 8A7. The reactivity of 8A7 in normal and neoplastic tissue was examined by performing immunohistochemistry on paraffin-embedded sections. 8A7 reacted with lymphocytes in the mantle and marginal zones, but not with lymphocytes in the interfollicular area. Lymphocytes in the germinal centers were found to be negative or occasionally weakly positive for 8A7. BAFF-R expression was found only in B-cell lymphoma (44/80, positive cases/examined cases): B-lymphoblastic lymphoma 0/3, B-chronic lymphocytic leukemia/small lymphocytic lymphoma 4/4, mantle cell lymphoma 9/11, follicular lymphoma 10/14, diffuse large B-cell lymphoma (DLBCL) 11/25, marginal zone B-cell lymphoma 8/10, lymphoplasmacytic lymphoma 2/2, plasma cell myeloma 0/2, and Burkitt lymphoma 0/9, but not in T/NK cell lymphomas (0/19) or Hodgkin lymphoma (0/10). BAFF-R was expressed in most low-grade B-cell neoplasms and a small number of DLBCL, suggesting that BAFF-R may play an important role in the proliferation of neoplastic lymphoid cells. Thus, the mAb is very useful for further understanding of both healthy B-cell biology and its pathogenic neoplasms.

Keywords BAFF · BAFF-R · Monoclonal antibody · Immunohistochemistry · B-cell lymphoma · Diffuse large B-cell lymphoma

N. Nakamura (✉) · S. Yoshida · M. Abe
Department of Pathology,
Fukushima Medical University,
Hikarigaoka-1,
Fukushima-shi, 960-1295, Japan
e-mail: nao@fmu.ac.jp
Tel.: +81-24-5484488
Fax: +81-24-5484488

H. Hase · D. Sakurai · T. Kobata
Department of Immunology,
Dokkyo University School of Medicine,
Tochigi, Japan

N. Tsukada · J. Takizawa · S. Aoki
First Department of Internal Medicine,
Niigata University Medical Hospital,
Niigata University,
Niigata, Japan

M. Kojima
Department of Pathology,
Dokkyo University School of Medicine,
Tochigi, Japan

S. Nakamura
Department of Pathology and Molecular Diagnostics,
Aichi Cancer Center,
Nagoya, Japan

Introduction

B-cell-activating factor of the tumor necrosis factor (TNF) family (BAFF), also known as BLyS, THANK, TALL-1 and zTNF4, is a fundamental survival factor for B-cells, and BAFF functionality is indispensable for B-cell maturation [13, 18, 27, 28]. BAFF is a trimeric membrane-bound or soluble factor and is expressed by monocytes, macrophages, neutrophils and dendritic cells. Whereas BAFF-deficient mice lack mature B-cells, BAFF-transgenic mice, characterized by overexpression of BAFF, have increased the number of B-cells and develop autoimmunity [3, 4, 9, 12]. In particular, transitional type 2 (T2) B-cells and marginal zone B-cells are expanded in BAFF-transgenic mice. BAFF blockade does not inhibit germinal center (GC) formation or somatic hypermutation of immunoglobulin (Ig) genes, indicating that BAFF is required for the normal maintenance of B-cells, but not for the initiation of the GC reaction, although B-cell maturation and mature functions are severely impaired [35]. Recently, it was reported that BAFF is directly involved in B cell malignancy [2, 7, 22, 23].

Three receptors for BAFF have been established: B-cell maturation antigen (BCMA), transmembrane activator and

calcium-modulator, and cyclophilin ligand interactor (TACI) and the BAFF-receptor (BAFF-R, also called BR3) [3, 14, 32, 33]. All three receptors are expressed on B-cells, while TACI is also expressed on activated T-cells [13]. Whereas TACI and BCMA are found to bind to a proliferation-inducing ligand (APRIL), BAFF-R binds only to BAFF [13, 32]. TACI is known to negatively control B-cell homeostasis and T-cell independent immune responses from evidence obtained from TACI deficient mice [30, 34, 37]. Although BCMA was recently reported to be essential for the survival of plasma cells [1, 24], mice lacking BCMA possess normal-appearing B lymphocyte compartments [27]. Thus, only BAFF-R is clearly a key receptor involved in the successful survival and maturation of B-cells [13]. However, the distribution of BAFF-R in normal and malignant human lymphoid tissue has not been made fully clear.

Only a few reports on BAFF-R in malignant B-cells have appeared to date. Briones et al. examined the BAFF binding activity in 43 cases of non-Hodgkin's lymphoma (NHL) with flow cytometry [2]. Although all cases of NHL express receptors for BAFF, BAFF-R expression was not specifically classified. Chronic lymphocytic leukemia/small lymphocytic lymphoma (CLL/SLL), mantle cell lymphoma (MCL), follicular center lymphoma, Burkitt lymphoma (BL) and diffuse large cell lymphoma were reported to express BAFF-R mRNA [7, 22], and multiple myeloma (MM) was reported to express cell surface BAFF-R [23].

In this investigation, we established the mouse anti-human BAFF-R monoclonal antibody (mAb) and examined its reactivity in normal and neoplastic lymphoid tissues using immunohistochemistry. We found a high degree of significance in its distribution in normal lymphoid tissue and low-grade B-cell neoplasms as well as in a small part of diffuse large B-cell lymphoma (DLBCL).

Materials and methods

Cell preparation and cell cultures

Human peripheral blood mononuclear cells were isolated from pooled healthy donors by Ficoll-Hypaque density-gradient centrifugation. After the depletion of monocytes by adherence to the plastic surface of the culture dishes, E rosette-negative populations were collected with 5% sheep erythrocytes and Ficoll-Hypaque. Purified B-cells were isolated by depleting the non B-cells using a B-cell isolation kit and auto MACS (Miltenyi Biotec, Auburn, Calif., USA). The resultant B-cell population was <2% $CD14^+$, <1% $CD3^+$, <2% $CD57^+$, and >95% $CD20^+$. All cultures were conducted in RPMI 1640 medium supplemented with 25 mM HEPES (*N*-2-hydroxyethylpiperazine-*N'*-2-ethanesulfonic acid), 10% fetal calf serum, 2 mM L-glutamine, 1 mM sodium pyruvate, 5.5×10^{-2} mM 2-mercaptoethanol, 100 IU/ml penicillin, and 100 IU/ml streptomycin (all from Invitrogen, Carlsbad, Calif., USA).

Antibodies and reagents

Polyclonal anti-human BAFF-R antibody (C-20), control mouse IgG2a, and FITC-labeled goat antibody to mouse IgG were purchased from Santa Cruz Biotechnology (Santa Cruz, Calif., USA), Sigma-Aldrich (St Louis, Mo., USA), and CALTAG (Burlingame, Calif., USA), respectively.

Establishment of human BAFF-R transfectant

To construct a human BAFF-R expression vector, a cDNA encoding full-length human BAFF-R protein (GenBank No. AF373846) was custom-synthesized (Takara, Shiga, Japan), inserted into pBluescript SK (+) (Stratagene, La Jolla, Calif., USA) at the *Eco*RI and *Bam*HI sites, and finally into the pBCMGSneo expression vector [8] at the *Xho*I and *Not*I sites (pBCMGS-BAFF-R). Murine pre-B-cells (cell line 300-19) were electroporated with pBCMGS-BAFF-R and stable transfectants were selected with G418 treatment. Cells with high-density BAFF-R were cloned with a fluorescence-activated cell sorter (FACS). The vector alone-transfected cells (mock) have been described previously [6].

Generation of anti-human BAFF-R mAb

A BALB/c mouse was immunized with human BAFF-R-expressing transfectant cells 3 times at 10-day intervals. Three days after the final immunization, the splenocytes were fused with NS-1 cells (purchased from Human Science Research Resources Bank), and HAT (hypoxanthine-aminopterin-thymidine) selection and cloning of hybridomas were performed simultaneously using a hybridoma cloning kit (ClonaCell-HY; StemCell Technologies, British Columbia, Canada). Anti-human BAFF-R designated 8A7 (mouse IgG2a, κ) was established.

Immunoblot analysis

PBS-washed cell pellets were resuspended with 0.5% SDS solution and boiled for 5 min. Proteins (5–8 μg) were separated with SDS-PAGE, transferred to an Immobilon-P membrane (Millipore, Billerica, Mass., USA), blocked with 5% skim milk, and immunoblotted with arbitrary Ab and HRP-labeled secondary Ab. The immunoblots were developed by using the enhanced chemiluminescent substrate (SuperSignal West Pico; Pierce Chemical Co., Rockford, Ill., USA) and visualized with a LumiVision analyzer (Taitec Co., Tokyo), as previously described [5].

Flow cytometric analysis

Flow cytometric analysis was performed using FACScalibur and the associated Cell Quest software (both from Becton Dickinson, San Jose, Calif., USA). FITC-labeled

goat antibody to mouse IgG was used as a second Ab. An isotype-matched mouse IgG2a control was used throughout the studies and always reacted with <5% of the cells.

Tissues and immunohistochemistry

Formalin-fixed paraffin-embedded tissues were used in this study. Tonsils resected due to chronic tonsillitis, lymph nodes resected due to non-neoplastic lymphadenopathy, spleens resected because of non-lymphoma and bone marrow clots without malignancy were used for the non-neoplastic lymphoid tissues. Neoplastic lymphoid tissues from 109 cases were used in this study and comprised the following: three cases of B-lymphoblastic lymphoma (B-LBL), four cases of CLL/SLL, 11 cases of MCL, 14 cases of follicular lymphoma (FL), 25 cases of DLBCL, ten cases of marginal zone B-cell lymphoma (MZBCL), two cases of Lymphoplasmacytic lymphoma (LPL), two cases of plasma cell myeloma (PCM), nine cases of BL, three cases of T-lymphoblastic lymphoma, four cases of angioimmunoblastic T-cell lymphoma, five cases of peripheral T-cell lymphoma, unspecified, two cases of adult T-cell lymphoma, one case of systemic anaplastic large cell lymphoma, four cases of NK/T cell lymphoma and ten cases of Hodgkin lymphoma (HL). All cases of CLL/SLL and MCL expressed CD5. Cyclin D1 was immunohistochemically detected in all but one case of MCL. FL consisted of four cases of grade 1, four cases of grade 2 and six cases of grade 3. All cases of FL expressed CD10. DLBCL included three cases with CD5 (+) CD10 (−), three cases with CD5 (−) CD10 (+) and 19 cases with CD5 (−) CD10 (−). HL consisted of three cases of nodular lymphocyte predominance Hodgkin lymphoma (NLP-HL), four cases of mixed cellularity classical Hodgkin lymphoma (MC-CHL) and three cases of nodular sclerosis classical Hodgkin lymphoma (NS-CHL).

The de-paraffinized tissue section was pre-treated in citrate buffer with microwave oven heating. The section was incubated with the primary antibody at 4°C overnight and then the streptavidin-biotin complex method (Dakocytomation, Kyoto, Japan) was used. Neoplasms with >10% positive cells were judged as positive.

Results

Establishment of the anti-human BAFF-R mAb, 8A7

To evaluate the role of the interactions between BAFF and BAFF-R in human B cell responses, we developed an anti-human BAFF-R mAb. For this purpose, we first estab-

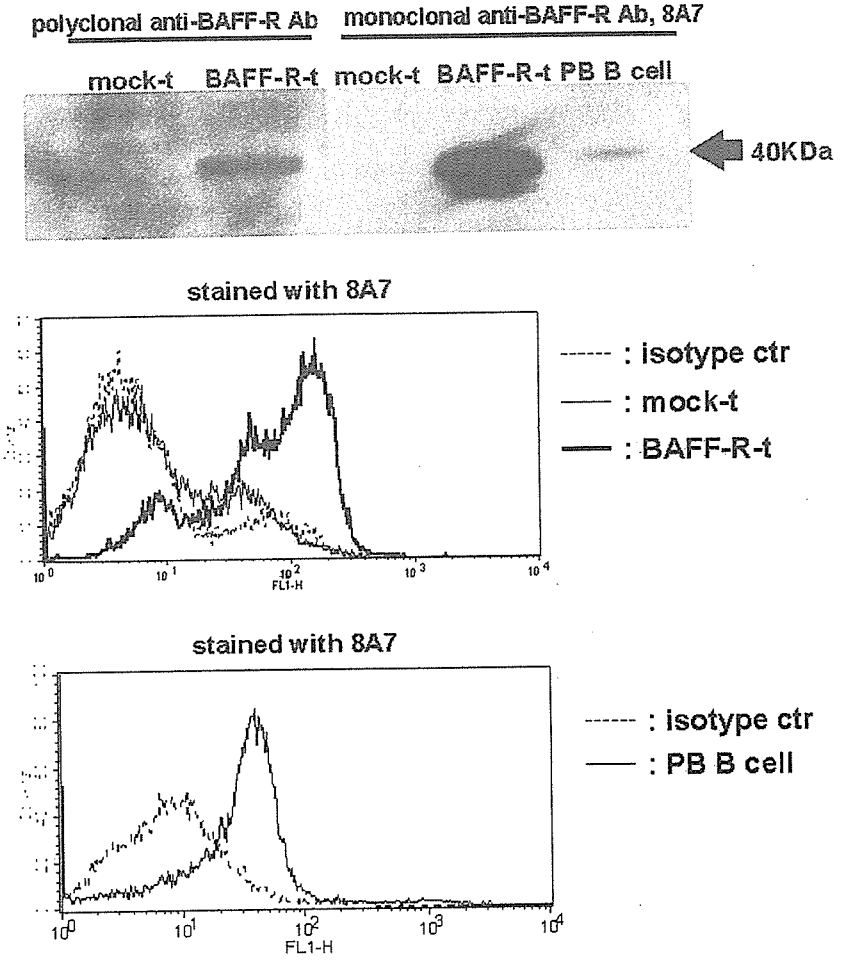

Fig. 1 8A7 mAb detects human BAFF-R. (a) Cell lysates prepared from BAFF-R- and mock-transfectants, and peripheral blood B cells, were subjected to immunoblot analysis using anti-human BAFF-R polyclonal Ab or 8A7 mAb. (b) Flow cytometric analysis of BAFF-R expression using 8A7 mAb. BAFF-R- and mock-transfectants and peripheral blood B cells were stained with 8A7 mAb or isotype-matched control Ab (IgG2a) followed by FITC-conjugated Ab to mouse IgG. Data shown are representative of three different experiments

lished a transfectant stably expressing human BAFF-R. Stable expression of human BAFF-R on the cDNA transfectant, but not on mock-transfected cells was verified using immunoblot analysis (Fig. 1a). Immunoblot analysis using commercially available polyclonal anti-human BA FF-R Ab revealed that BAFF-R cDNA-transfected cells expressed the BAFF-R molecule. We then immunized a BALB/c mouse with the BAFF-R-transfectant and fused the splenocytes with NS-1 myeloma cells. The hybridomas producing anti-human BAFF-R mAb were screened for specific reactivity to the BAFF-R-transfectant. As shown in Fig. 1a, one obtained mAb, designated 8A7, bound to BAFF-R-transfectant and peripheral blood B cells but not to mock-transfectant. Flow cytometric analysis revealed that the 8A7 mAb reacted with almost all peripheral blood B cells and BAFF-R-transfectant, but not with peripheral blood T-cells, monocytes, or mock-transfectant (Fig. 1b, data not shown).

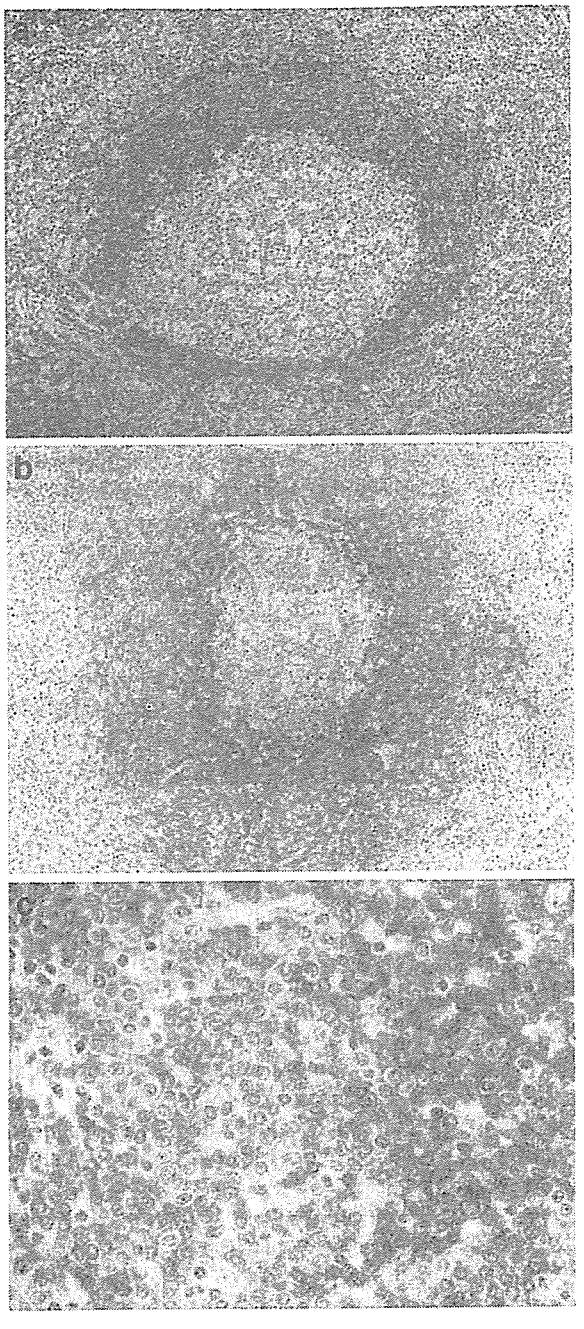

Fig. 2 BAFF-R expression in normal lymphoid tissues according to immunohistochemistry (IHC) on the paraffin-embedded section (strept/ABC method). 8A7 reacts with lymphocytes in the mantle zone of the secondary lymphoid follicles in the lymph node (**a**: IHC, original magnification ×50) and with lymphocytes in the mantle and marginal zones of the splenic white pulp (**b**: IHC, ×50). Marginal B-cells with a clear cytoplasm are positive for 8A7 (**c**: IHC, ×200)

Immunohistochemistry of non-neoplastic lymphoid tissue

8A7 reacted with lymphocytes in the mantle zone of the secondary lymphoid follicles in the tonsil (Fig. 2a) and the non-neoplastic lymph nodes. In the spleen, 8A7 reacted with lymphocytes in the mantle and marginal zones of the white pulp, but not with the interfollicular area (Fig. 2b,c). Lymphocytes in germinal centers (GCs) were found to be negative or occasionally weakly positive for hyperplastic GC. 8A7 failed to stain hematopoietic cells in the bone marrow. Plasma cells were negative for 8A7.

Immunohistochemistry of the neoplastic lymphoid tissue

Expression of BAFF-R in neoplastic lymphoid tissue detected by 8A7 is shown in Table 1 and Fig. 3. BAFF-R expression was only found in B-cell lymphoma (44/80, positive cases/examined cases), but not in T/NK cell lymphoma (0/19) or in Hodgkin lymphoma (0/10).

Discussion

An anti-human BAFF-R mAb, named 8A7, was developed using a transfectant stably expressing human BAFF-R to evaluate the role of interactions between BAFF and BAFF-R in human B-cell responses and malignancy. In this paper, reactivity and distribution in normal and malignant lymphoid tissues was addressed by means of immunohistochemistry with paraffin-embedded tissue.

The distribution of BAFF-R in human lymphoid tissue has not been heretofore reported, except in a recent report by Ng et al. [21]. They stated that the BAFF-R was expressed at a high level on all B-cells and at very low levels on T-cells in human peripheral blood. It is also expressed in tonsil B-cells, but B-cells with a GC phenotype ($CD38^+$, $CD27^+$, $CD39^-$, $CD24^-$ and IgM^-) exhibited lower levels of BAFF-R according to flow cytometry [21]. Intense staining of B-cell follicles and weaker staining of the GCs were observed in the immunohistochemistry using frozen sections [21]. We demonstrated that BAFF-R was strongly expressed on B-cells situated both in the mantle zone and the marginal zones of the secondary lymphoid follicles and weakly expressed on GC B-cells occasionally

Table 1 Reactivity of 8A7 in 109 neoplastic lymphoid tissues according to immunohistochemistry (Positive cases/examined cases). *NLP-HL* nodular lymphocyte predominance Hodgkin lymphoma; *MC-CHL* mixed cellularity classical Hodgkin lymphoma; *NS-CHL* nodular sclerosis classical Hodgkin lymphoma

B-lymphoblastic lymphoma	0/3
Chronic lymphocytic leukemia/Small lymphocytic lymphoma	4/4
Mantle cell lymphoma	9/11
Follicular lymphoma	10/14
Grade 1	4/4
Grade 2	4/4
Grade 3	2/6
Diffuse large B-cell lymphoma	11/25
Marginal zone B-cell lymphoma	8/10
Lymphoplasmacytic lymphoma	2/2
Plasma cell myeloma	0/2
Burkitt lymphoma	0/9
T-lymphoblastic lymphoma	0/3
Angioimmunoblastic T-cell lymphoma	0/4
Peripheral T-cell lymphoma, unspecified	0/5
Adult T-cell lymphoma	0/2
Anaplastic large cell lymphoma	0/1
NK/T cell lymphoma	0/4
Hodgkin lymphoma	0/10
NLP-HL	0/3
MC-CHL	0/4
NS-CHL	0/3

in the GCs. The intensity of BAFF-R in GC B-cells may vary between each GC. Marginal zone B-cells have somatically hypermutated immunoglobulin (Ig) genes and express CD27 at a level equivalent to memory B-cells [10]. It is widely considered that marginal zone B-cell development and survival are likely to directly or indirectly depend on BAFF [13]. Since the present data indicate that marginal B-cells express BAFF-R, it is likely that BAFF directly contributes to the maturation of marginal zone B-cells. BAFF-R was also expressed strongly on mantle zone B-cells, which are naive B-cells that exhibit unmutated Ig genes and mainly co-express IgM and IgD [11]. On the other hand, GC B-cells that undergo affinity maturation of their antigen receptors and express CD10 and CD38 [25] were observed to be negative or weakly positive for BAFF-R. Thus, BAFF-R is widely distributed on un-stimulated B-cells and antigen-stimulated B-cells during B cell differentiation, except for GC B-cells. This pattern of BAFF-R expression during different stages of B-cell differentiation seemed to be similar to that of Bcl-2 expression. GC B-cells express low levels of BAFF-R and the anti-apoptotic factor Bcl-2, and high levels of the apoptotic factor Fas [17, 39].

Novak et al. reported the cell surface expression of BAFF-R on both CD5 (+) peripheral blood B-cells as well as CD5 (−) peripheral blood B-cells [23]. Mice transgenic for TACI-Ig, and BAFF-deficient mice display a developmental block of B-cell maturation in the periphery, leading to a severe depletion of marginal zone and follicular B2 B-cells, but not of peritoneal CD5 (+) B1 B-cells [4, 13, 29]. Interactions between BAFF and BAFF-R may be needed for CD5 (+) B1 B-cell maturation as much as CD5 (−) B2 B-cell maturation in humans.

The reactivity of anti-BAFF-R mAb against neoplastic lymphoid tissue is of considerable interest. It is likely that BAFF-R expression was only found in B-cell lymphoma, but not in T/NK-cell lymphomas, for reasons related to the fact that BAFF-R expression is normally found only on healthy B-cells [21]. Only a small number of studies reporting BAFF-R expression in malignant B-cells have appeared to date. Seven of seven B-CLL samples, as well as normal B-cells, expressed BAFF-R mRNA [22]. None of the five MM cell-lines but two of the three mononuclear cells of patients with MM expressed cell surface BAFF-R [23]. Six of six NHLs, including CLL/SLL, MCL, FL, BL, and DLBCL, expressed BAFF-R mRNA [7]. In the present study, however, we demonstrated somewhat different results for BAFF-R expression.

Most of the low-grade B-cell neoplasms of B-CLL/SLL, MCL, LPL and MZBCL strongly exhibited BAFF-R. Among them, MCL and MZBCL are believed to be neoplasms derived from mantle zone B-cells and marginal zone B-cells, respectively. The normal counterpart cells of B-CLL/SLL are a neoplasm of CD5 (+) B-cells of the peripheral blood [15, 29]. These normal counterpart cells are all BAFF-R (+) and these B-cell neoplasms seemed to maintain BAFF-R expression. Low-grade B-cell lymphomas may require the interaction of BAFF and BAFF-R for survival and proliferation of the neoplastic B-cells.

Although normal GC B-cells exhibited a negative reaction or an occasionally weakly positive reaction for 8A7, both grade 1 and 2 FLs strongly expressed BAFF-R. FL consists of small-cleaved lymphoma cells with intermingled large sized centroblasts. Grade 1 and 2 FLs include less than 50 centroblasts and 50–150 centroblasts per ten high-power fields, respectively. Both grades 1 and 2 FLs retain a follicular growth pattern supported by a network of follicular dendritic cells (FDCs), and the lymphoma cells express CD20, CD10, Bcl-2 and Bcl-6 [20]. It has recently been shown that FDCs express BAFF [6]. On the other hand, in grade 3 FL, 2/3 in grade 3a and 0/3 in grade 3b were positive for 8A7. This may indicate that lymphoma cells of grade 1 and 2 FLs require the interaction of BAFF and BAFF-R for their survival and growth. Certain lymphoma cells of some grade 3 FL act autonomically in terms of proliferation.

BAFF-R was expressed in a lower number of cases of aggressive B-cell lymphomas. LBL and BL were negative for 8A7. Eleven out of 25 DLBCLs exhibited a positive reaction with anti-BAFF-R mAb, which supports the recent report by He et al. [7]. Among these, the expression of BAFF-R was found in CD5 (+) DLBCL as well as CD5 (+) CLL/SLL and MCL. BAFF-R (+) in many cases of CD5 (+) B-cell neoplasms was independent of their aggressiveness and clinical behavior. These findings may prove to be useful for the continual improvement of understanding of the biology of CD5 (+) B-cells and B-cell neoplasms, especially for CD5 (+) DLBCL, which is reported to have a poorer clinical outcome than CD5 (−) DLBCL [19, 36].

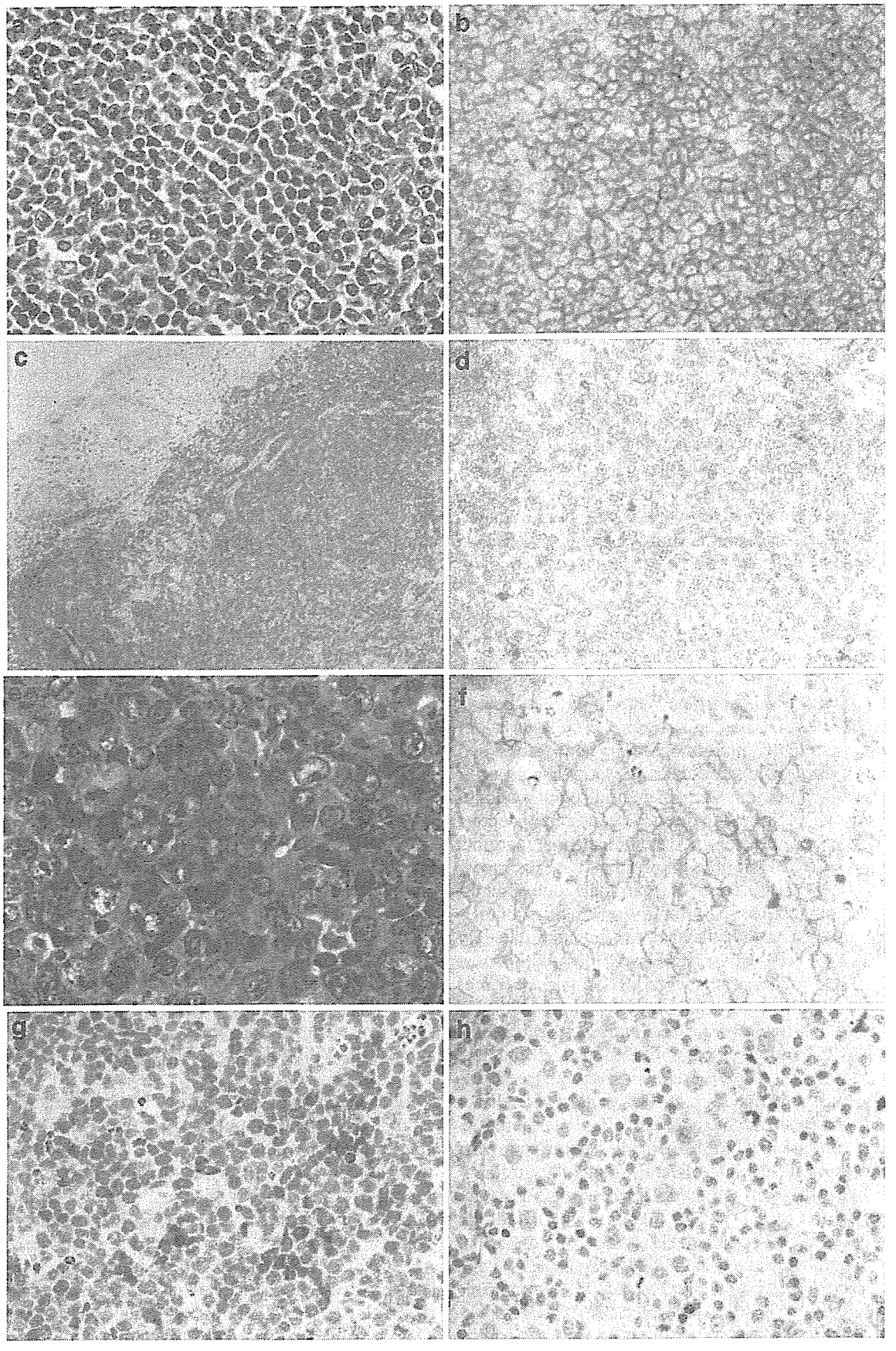
a
b
c
d
f
g
h

◀ **Fig. 3** BAFF-R expression in neoplastic lymphoid tissues according to immunohistochemistry (IHC) on the paraffin-embedded sections (strept/ABC method). 8A7 is strongly expressed in CD20 (+) CD5 (+) cyclin D1 (+) mantle cell lymphoma (**a**: HE, **b**: IHC, original magnification ×200). 8A7 reacts with the lymphoma cells of gastric MALT lymphoma, but not with the glandular epithelium (**c**: IHC, ×50; **d**: IHC, ×200). 8A7 expressed on some of the lymphoma cells of CD20 (+) CD5 (+) diffuse large B-cell lymphoma (**e**: HE, **f**: IHC, ×200) (**g**: IHC, ×200). Expression of 8A7 is not found in Hodgkin/Reed-Sternberg cells of Hodgkin lymphoma, but in a small number of small lymphocytes (**h**: IHC, ×200) Burkitt lymphoma is negative for 8A7

We analyzed the clinical profiling between BAFF-R (+) and BAFF-R (−) subgroups in all DLBCL examined. When analyzing these between the BAFF-R (+) and BA FF-R (−) subgroups in CD5 (−) CD10 (−) DLBCL, we found a significant difference in LDH. The number of patients with LDH >2-fold of the normal limit in the BAFF-R (+) subgroups was greater than that in the BAFF-R (−) subgroup (detailed data not shown). This may mean that the volume of lymphoma cells in patients with BAFF-R (+) DLBCL is high and may affect the treatment strategy for patients with BAFF-R (+) DLBCL. We found no significant differences in the overall survival curves between the two subgroups due to the small number of patients in this study, and more cases are needed for an accurate estimation. BAFF-R is a possible marker for sub-grouping of DLBCL. On the other hand, two out of three CD5 (+) DLBCL exhibited more than 2-fold the normal limit of LDH, but both cases of CD10 (+) DLBCL exhibited LDH within the normal limit.

The HRS cells of all cases of HL including NLP-HL, MC-CHL and NS-CHL were negative for BAFF-R. This is a marked difference from the finding that more than half of HL cases express the bcl-2 protein, an anti-apoptotic factor [26]. HL is a neoplasm derived from GC B-cells with a hypermutated Ig gene, as disclosed by single cell PCR analysis, and lacks Ig mRNA, which is different from the cases of DLBCL [16, 38]. Since the expression of BAFF-R is regulated by immunoglobulin, it is possible that HL is not able to express BAFF-R [31]. It is, however, odd that the NLP-HL that expresses Ig was also negative for 8A7.

In conclusion, we developed an anti-human BAFF-R mAb and addressed its reactivity and distribution in normal and malignant lymphoid tissues by performing immunohistochemistry with paraffin-embedded tissues. BAFF-R was found to be expressed on B-cells situated in the mantle and marginal zones, but not on B-cells in GC. We demonstrated that BAFF-R was expressed on most low-grade B-cell neoplasms and in some DLBCL.

Acknowledgements We thank Dr. Hajime Karasuyama for the pBCMGSneo expression vector, Dr. Hidefumi Kojima for helpful discussion, and Ms. Yumiko Kanno for participating in technical assistance. We also thank the Laboratory Animal Research Center and the Laboratory of Analytical Instruments, Institute for Medical Science, Dokkyo University School of Medicine, for the use of their facilities.

A grant-in-aid for Scientic Research (c) from the Ministry of Education, Culture, Sports, Science and Technology of Japan (KA KENHI 16590410 to T.K.) and The Science Research Promotion Fund from the Promotion and Mutual Aid Corporation for Private Schools of Japan (to T.K.)

References

1. Avery DT, Kalled SL, Ellyard JI et al (2003) BAFF selectively enhances the survival of plasmablasts generated from human memory B cells. J Clin invest 112:286–297
2. Briones J, Timmerman JM, Hilbert DM, Levy R (2002) BLyS and BlyS receptor expression in non-Hodgkin's lymphoma. Exp Hematol 30:135–141
3. Gross JA, Johnston J, Mudri S, Enselman R, Dillon SR, Madden K, Xu W, Parrish-Novak J, Foster D, Lofton-Day C, Moore M, Littau A, Grossman A, Haugen H, Foley K, Blumberg H, Harrison K, Kindsvogel W, Clegg CH (2000) TACI and BCMA are receptors for a TNF homologue implicated in B-cell autoimmune disease. Nature 404:995–999
4. Gross JA, Dillon SR, Mudri S, Johnston J, Littau A, Roque R, Rixon M, Schou O, Foley KP, Haugen H, McMillen S, Waggie K, Schreckhise RW, Shoemaker K, Vu T, Moore M, Grossman A, Clegg CH (2001) TACI-Ig neutralizes molecules critical for B cell development and autoimmune disease. Impaired B cell maturation in mice lacking BLyS. Immunity 15:289–302
5. Hase H, Kanno Y, Kojima H, Morimoto C, Okumura K, Kobata T (2002) CD27 and CD40 inhibit p53-independent mitochondrial pathways in apoptosis of B cells induced by B cell receptor ligation. J Biol Chem 277:46950–46958
6. Hase H, Kanno Y, Kojima M, Hasegawa K, Sakurai D, Kojima H, Tsuchiya N, Tokunaga K, Masawa N, Azuma M, Okumura K, Kobata T (2004) BAFF/BLyS can potentiate B-cell selection with the B-cell co-receptor complex. Blood 103:2257–2265
7. He B, Chadburn A, Jou E, Schattner EJ, Knowles DM, Cerutti A (2004) Lymphoma B cells evade apoptosis through the TNF family members BAFF/BLyS and APRIL. J Immunol 172:3268–3279
8. Karasuyama H, Kudo A, Melcher F (1990) The proteins encoded by the VpreB and lambda 5 pre-B cell-specific genes can associate with each other and with mu heavy chain. J Exp Med 172:969–972
9. Khare SD, Sarosi I, Xia XZ, McCabe S, Miner K, Solovyev I, Hawkins N, Kelley M, Chang D, Van G, Ross L, Delaney J, Wang L, Lacey D, Boyle WJ, Hsu H (2000) Severe B cell hyperplasia and autoimmune disease in TALL-1 transgenic mice. Proc Natl Acad Sci USA 97:3370–3375
10. Klein U, Rajewsky K, Kuppers R (1998) Human immunoglobulin (Ig)M+IgD+ peripheral blood B cells expressing the CD27 cell surface antigen carry somatically mutated variable region genes: CD27 as a general marker for somatically mutated (memory) B cells. J Exp Med 188:1679–1689
11. Klein U, Goossens T, Fischer M, Kanzler H, Braeuninger A, Rajewsky K, Kuppers R (1998) Somatic hypermutation in normal and transformed human B cells. Immunol Rev 162:261–280
12. Mackay F, Woodcock SA, Lawton P et al. (1999) Mice transgenic for BAFF develop lymphocytic disorders along with autoimmune manifestations. J Exp Med 190:1697–1710
13. Mackay F, Schneider P, Rennert P, Browning JL (2003) BAFF and APRIL: a tutorial on B cell survival. Annu Rev Immunol 21:231–264
14. Madry C, Laabi Y, Callebaut I et al. (1988) The characterization of murine BCMA gene defines it as a new member of the tumor necrosis factor superfamily. Int Immunol 10:1063–1702
15. Maes B, De Wolf-Peeters C (2002) Marginal zone cell lymphoma—an update on recent advances. Histopathology 40:117–126
16. Marafioti T, Hummel M, Foss HD, Laumen H, Korbjuhn P, Anagnostopoulos I, Lammert H, Demel G, Theil J, Wirth T, Stein H (2000) Hodgkin and Reed-Sternberg cells represent an expansion of a single clone originating from a germinal center B-cell with functional immunoglobulin gene rearrangements but defective immunoglobulin transcription. Blood 95:1443–1450

17. Martinez-Valdez H, Guret C, de Bouteiller O, Fugier I, Banchereau J, Liu YJ (1996) Human germinal center B cells express the apoptosis-inducing genes Fas, c-myc, P53, and Bax but not the survival gene bcl-2. J Exp Med 183:971–977
18. Moore PA, Belvedere O, Orr A, Pieri K, LaFleur DW, Feng P, Soppet D, Charters M, Gentz R, Parmelee D, Li Y, Galperina O, Giri J, Roschke V, Nardelli B, Carrell J, Sosnovtseva S, Greenfield W, Ruben SM, Olsen HS, Fikes J, Hilbert DM (1999) BLyS: member of the tumor necrosis factor family and B lymphocyte stimulator. Science 285:260–263
19. Nakamura N, Abe M (2003) Histogenesis of CD5-positive and CD5-negative B-cell neoplasms on the aspect of somatic mutation of immunoglobulin heavy chain gene variable region. Fukushima J Med Sci 49:55–67
20. Nathwani BN, Harris NL, Weisenburger D, Isaacson PG, Piris MA, Berger F, Muller-Hermalink HK, Swerdlow SH (2001) Follicular lymphoma. In: Jaffe ES, Harris NL, Stein H, Vardiman JW (eds) Tumours of haematopoietic and lymphoid tissues. IARC Press, Lyon, France pp 162–167
21. Ng LG, Sutherland AP, Newton R, Qian F, Cachero TG, Scott ML, Thompson JS, Wheway J, Chtanova T, Groom J, Sutton IJ, Xin C, Tangye SG, Kalled SL, Mackay F, Mackay CR (2004) B cell-activating factor belonging to the TNF family (BAFF)-R is the principal BAFF receptor facilitating BAFF costimulation of circulating T and B cells. J Immunol 173:807–817
22. Novak AJ, Bram RJ, Kay NE, Jelinek DF (2002) Aberrant expression of B-lymphocyte stimulator by B chronic lymphocytic leukemia cells: a mechanism for survival. Blood 100: 2973–2979
23. Novak AJ, Darce JR, Arendt BK, Harder B, Henderson K, Kindsvogel W, Gross JA, Greipp PR, Jelinek DF (2004) Expression of BCMA, TACI, and BAFF-R in multiple myeloma: a mechanism for growth and survival. Blood 103:689–694
24. O'Connor BP, Raman VS, Erickson LD, Cook WJ, Weaver LK, Ahonen C, Lin L-L, Mantchev GT, Bram RJ, Noelle RJ (2004) BCMA is essential for the survival of long-lived bone marrow plasma cells. J Exp Med 199:91–97
25. Pascual V, Liu YJ, Magalski A, de Bouteiller O, Banchereau J, Capra JD (1994) Analysis of somatic mutation in five B cell subsets of human tonsil. J Exp Med 180:329–339
26. Rassidakis GZ, Medeiros LJ, Vassilakopoulos TP, Viviani S, Bonfante V, Nadali G, Herling M, Angelopoulou MK, Giardini R, Chilosi M, Kittas C, McDonnell TJ, Bonadonna G, Gianni AM, Pizzolo G, Pangalis GA, Cabanillas F, Sarris AH (2002) BCL-2 expression in Hodgkin and Reed-Sternberg cells of classical Hodgkin disease predicts a poorer prognosis in patients treated with ABVD or equivalent regimens. Blood 100:3935–3941
27. Schiemann B, Gommerman JL, Vora K, Cachero TG, Shulga-Morskaya S, Dobles M, Frew E, Scott ML (2001) An essential role for BAFF in the normal development of B cells through a BCMA-independent pathway. Science 293:2111–2114
28. Schneider P, MacKay F, Steiner V, Hofmann K, Bodmer JL, Holler N, Ambrose C, Lawton P, Bixler S, Acha-Orbea H, Valmori D, Romero P, Werner-Favre C, Zubler RH, Browning JL, Tschopp J (1999) BAFF, a novel ligand of the tumor necrosis factor family, stimulates B cell growth. J Exp Med 189:1747–1756
29. Schneider P, Takatsuka H, Wilson A, Mackay F, Tardivel A, Lens S, Cachero TG, Finke D, Beermann F, Tschopp J (2001) Maturation of marginal zone and follicular B cells requires B cell activating factor of the tumor necrosis factor family and is independent of B cell maturation antigen. J Exp Med 194:1691–1697
30. Seshasayee D, Valdez P, Yan M, Dixit VM, Tumas D, Grewal IS (2003) Loss of TACI causes fatal lymphoproliferation and autoimmunity, establishing TACI as as inhibitory BLys receptor. Immunity 18:279–288
31. Smith SH, Cancro MP (2003) Cutting edge: B cell receptor signals regulate BLyS receptor levels in mature B cells and their immediate progenitors. J Immunol 170:5820–5823
32. Thompson JS, Bixler SA, Qian F et al. (2001) BAFF-R, a newly identified TNF receptor that specifically interacts with BAFF. Science 293:2108–2111
33. von Bulow GU, Bram RJ (1997) NF-AT activation induced by a CAML-interacting member of the tumor necrosis factor superfamily. Science 278:138–141
34. von Bulow GU, van Deursen JM, Bram RJ (2001) Regulation of the T-independent humoral response by TACI. Immunity 14: 573–582
35. Vora KA, Wang LC, Rao SP, Liu ZY, Majeau GR, Cutler AH, Hochman PS, Scott ML, Kalled SL (2003) Germinal centers formed in the absence of B cell-activating factor belonging to the TNF family exhibit impaired maturation and function. J Immunol 171:547–551
36. Yamaguchi M, Seto M, Okamoto M, Ichinohasama R, Nakamura N, Yoshino T, Suzumiya J, Murase T, Miura I, Akasaka T, Tamaru J, Suzuki R, Kagami Y, Hirano M, Morishima Y, Ueda R, Shiku H, Nakamura S (2002) De novo CD5+ diffuse large B-cell lymphoma: a clinicopathologic study of 109 patients. Blood 99:815–821
37. Yan M, Wang H, Chan B et al. (2001) Activation and accumulation of B-cells in TACI-deficient mice. Nat Immunol 2:638–645
38. Yatabe Y, Oka K, Asai J, Mori N (1996) Poor correlation between clonal immunoglobulin gene rearrangement and immunoglobulin gene transcription in Hodgkin's disease. Am J Pathol 149:1351–1361
39. Yoshino T, Kondo E, Cao L, Takahashi K, Hayashi K, Nomura S, Akagi T (1994) Inverse expression of bcl-2 protein and Fas antigen in lymphoblasts in peripheral lymph nodes and activated peripheral blood T and B lymphocytes. Blood 83:1856–1861

JOURNAL OF VIROLOGY, Feb. 2005, p. 2087–2096 Vol. 79, No. 4
0022-538X/05/$08.00+0 doi:10.1128/JVI.79.4.2087–2096.2005

Potent Anti-R5 Human Immunodeficiency Virus Type 1 Effects of a CCR5 Antagonist, AK602/ONO4128/GW873140, in a Novel Human Peripheral Blood Mononuclear Cell Nonobese Diabetic-SCID, Interleukin-2 Receptor γ-Chain-Knocked-Out AIDS Mouse Model

Hirotomo Nakata,[1] Kenji Maeda,[1] Toshikazu Miyakawa,[1] Shiro Shibayama,[2] Masayoshi Matsuo,[2] Yoshikazu Takaoka,[2] Mamoru Ito,[3] Yoshio Koyanagi,[4]† and Hiroaki Mitsuya[1,5]*

Department of Infectious Diseases, Kumamoto University Graduate School of Medicine, Kumamoto,[1] Ono Pharmaceutical Co. Ltd., Osaka,[2] Central Institute for Experimental Animals, Kawasaki,[3] Department of Virology, Tohoku University Graduate School of Medicine, Sendai,[4] Japan, and Experimental Retrovirology Section, HIV and AIDS Malignancy Branch, National Cancer Institute, Bethesda, Maryland[5]

Received 27 May 2004/Accepted 1 October 2004

We established human peripheral blood mononuclear cell (PBMC)-transplanted R5 human immunodeficiency virus type 1 isolate JR-FL (HIV-1_{JR-FL})-infected, nonobese diabetic-SCID, interleukin 2 receptor γ-chain-knocked-out (NOG) mice, in which massive and systemic HIV-1 infection occurred. The susceptibility of the implanted PBMC to the infectivity and cytopathic effect of R5 HIV-1 appeared to stem from hyperactivation of the PBMC, which rapidly proliferated and expressed high levels of CCR5. When a novel spirodiketopiperazine-containing CCR5 inhibitor, AK602/ONO4128/GW873140 (molecular weight, 614), was administered to the NOG mice 1 day after R5 HIV-1 inoculation, the replication and cytopathic effects of R5 HIV-1 were significantly suppressed. In saline-treated mice ($n = 7$), the mean human $CD4^+/CD8^+$ cell ratio was 0.1 on day 16 after inoculation, while levels in mice ($n = 8$) administered AK602 had a mean value of 0.92, comparable to levels in uninfected mice ($n = 7$). The mean number of HIV-RNA copies in plasma in saline-treated mice were $\sim 10^6$/ml on day 16, while levels in AK602-treated mice were 1.27×10^3/ml ($P = 0.001$). AK602 also significantly suppressed the number of proviral DNA copies and serum p24 levels ($P = 0.001$). These data suggest that the present NOG mouse system should serve as a small-animal AIDS model and warrant that AK602 be further developed as a potential therapeutic for HIV-1 infection.

Highly active antiretroviral therapy has brought about a major impact on the AIDS epidemics in the industrially advanced nations (5, 22). However, eradication of human immunodeficiency virus type 1 (HIV-1) is thought to be currently impossible, due in part to the viral reservoirs remaining in blood and infected tissues (6). The limitation of antiviral therapy of AIDS is exacerbated by complicated regimens, the development of drug-resistant HIV-1 variants (11), and a number of inherent adverse effects (2, 31). Hence, the identification of new antiretroviral drugs that have unique mechanisms of action and produce no or minimal adverse effects remains an important therapeutic objective. In regard to development of potential anti-HIV therapies or vaccines, experimental animal models for AIDS which allow the determination of the possible efficacy of antiviral agents or vaccines have been sought since severe combined immunodeficiency (SCID) mice engrafted with human fetal thymus, liver, or peripheral blood mononuclear cells (PBMC) were first exploited to examine antiretroviral agents (19, 25). However, a number of mouse models have suffered from false-positive and false-negative results in detecting or quantifying HIV-1 infection and replication and have required a large number of samples and mice for testing (25, 29).

In the present work, we established human PBMC-transplanted R5 HIV-1_{JR-FL}-infected, nonobese diabetic (NOD)-SCID, interleukin 2 receptor γ (IL-2Rγ)-chain-knocked-out (NOG) mice, in which massive and systemic HIV-1 infection occurs, human $CD4^+/CD8^+$ cell ratios significantly decrease, and high levels of R5 HIV-1 viremia reaching as high as 10^6 copies/ml are achieved. Furthermore, we demonstrated that this unprecedented susceptibility of the implanted human PBMC to the infectivity and cytopathic effects of R5 HIV-1 infection stems from hyperactivation of the PBMC. Here, we also report a novel small nonpeptide CCR5 antagonist, AK602/ONO4128/GW873140, which exerts potent anti-HIV-1 activity in vitro against laboratory and clinical strains of HIV-1, including highly multidrug-resistant (MDR) variants.

* Corresponding author. Mailing address: Department of Infectious Diseases, Kumamoto University Graduate School of Medicine, 1-1-1 Honjo, Kumamoto 860-8556, Japan. Phone: 81-96-373-5156. Fax: 81-96-363-5265. E-mail: hmitsuya@helix.nih.gov.

† Present address: Laboratory of Viral Pathogenesis, Institute for Virus Research, Kyoto University, Kyoto 606-8507, Japan.

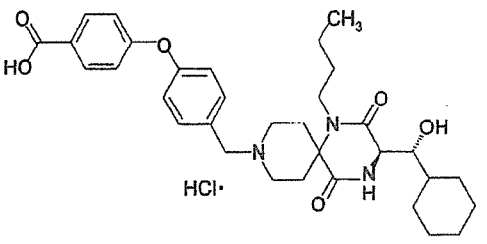

FIG. 1. Structure of AK602.

MATERIALS AND METHODS

Transplantation of human PBMC in NOG mice. NOD-SCID (NOG) mice (10, 33) were maintained in the Central Institute for Experimental Animals (Kawasaki, Japan). Mice were 4 to 6 weeks old at the time of transfer of human PBMC. The human PBMC-transplanted NOG (hu-PBMC-NOG) mice were generated by methods previously described (23, 24). Briefly, PBMC (10^7) were freshly prepared from heparinized blood of a single healthy HIV-1-seronegative donor by Ficoll-Hypaque density gradient centrifugation, resuspended in RPMI 1640-based culture medium (0.5 ml), and infused intraperitoneally to each mouse. The experimental protocol was approved by the Ethics Review Committees for Animal Experimentation of the participating institutions.

Assay for proliferation and CCR5 expression of transplanted human PBMC recovered from hu-PBMC-NOG mice. Freshly isolated human PBMC (2×10^7 cells/ml) were incubated in phosphate-buffered saline (PBS) containing 10 μM 5-carboxyfluorescein diacetate succinimidyl ester (CFSE; Molecular Probes, Eugene, Oreg.) for 15 min at 37°C for CFSE labeling as previously described by Lyons (16), washed, and resuspended in RPMI 1640. One part of the labeled PBMC preparation was intraperitoneally injected (10^7 PBMC) to each NOG mouse, and human PBMC were recovered from peritoneal lavages and spleen. The other part of the preparation was immediately stimulated with 10 μg of phytohemagglutinin (PHA)/ml, cultured, and harvested. PBMC samples thus obtained were labeled with phycoerythrin (PE)-conjugated anti-CCR5 monoclonal antibody 3A9 or peridinin chlorophyll protein-conjugated anti-HLA-DR antibody (BD Pharmingen, San Diego, Calif.) and subjected to flow cytometric analysis with a Becton Dickinson FACscan cytometer; the data were analyzed by Cell Quest software (Becton Dickinson, Franklin Lakes, N.J.). A quantitative fluorescence-activated cell sorting (FACS) assay that relies on a series of precalibrated beads that bind to a fixed number of mouse immunoglobulin G molecules (Quantum Simply Cellular Kit; Sigma, Saint Louis, Mo.) to determine the absolute number of CCR5s on the cell surface was also conducted according to the manufacturer's instructions (15).

Cells and viruses. The HeLa-CD4-LTR-β-gal indicator cell line expressing human CCR5 ($CCR5^+$ MAGI) (18), a kind gift from Yosuke Maeda, was used for the present study. 293T cells (a human embryonic kidney cell line) were cultured in Dulbecco's modified Eagle medium supplemented with 10% fetal calf serum (FCS) and antibiotics and used for transfection of DNA plasmid containing the R5 HIV-$1_{JR\text{-}FL}$ genome (13). PBMC isolated from HIV-1-seronegative individuals were cultured with 10% FCS and antibiotics with 10 μg of PHA/ml for 3 days prior to anti-HIV-1 activity assay in vitro (PHA-PBMC). A panel of HIV-1 strains was employed for the drug susceptibility attempt: HIV-$1_{Ba\text{-}L}$ (7), HIV-$1_{JR\text{-}FL}$ (13), HIV-$1_{NL4\text{-}3}$ (32), a wild-type HIV-1_{MOKW} isolated from a drug-naive AIDS patient (17), and MDR primary HIV-1 (HIV-1_{MDR}) strain (HIV-1_{JSL} and HIV-1_{MM}) (35). All primary HIV-1 strains were passaged once or twice in PHA-PBMC cultures and the culture supernatants were stored at −80°C until use. Antiviral assays using PHA-PBMC were conducted as previously reported (12, 17, 35).

Antiviral agents and assay for inhibition of R5 HIV-1 infectivity and replication. A series of different spirodiketopiperazine (SDP) derivatives were newly designed, synthesized, and tested for their activity against in vitro infectivity and replication of R5 HIV-1 as previously described (17). AK602 was chosen for this study based on its CCR5-specific, potent activity against R5 HIV-1. A method for the synthesis of AK602 will be published elsewhere. The structure of AK602 is illustrated in Fig. 1. An approved drug for therapy for HIV-1 infection, 2′,3′-dideoxyinosine (ddI) (20, 21), was kindly provided by Ajinomoto Co., Inc. Tokyo, Japan. TAK779 and SCH-C were synthesized according to previously published data (1, 30). The MAGI assay using $CCR5^+$ MAGI cells was conducted as previously described (17) with minor modifications. Briefly, $CCR5^+$ MAGI cells were seeded in 96-well, flat-bottomed microculture plates (10^4 cells/well) for 24 h, exposed to 0.1 or 1 μM AK602 for 30 min, washed three times, exposed to R5 HIV-1 (100 50% tissue culture infectious doses) at various time points after AK602 removal, and cultured in Dulbecco's modified Eagle medium containing 15% FCS for 48 h. Following the removal of supernatants and lysis of the cells with PBS (100 μl) containing 1% Triton X-100, a solution (100 μl) containing 10 mM chlorophenol red-β-D-galactopyranoside, 2 mM $MgCl_2$, and 0.1 M KH_2PO_4 was added to each well; the mixture was incubated at room temperature in the dark for 30 min; and the optical density (wavelength, 570 nm) was measured with a microplate reader (*V*max, Molecular Devices, Sunnyvale, Calif). All assays were performed in triplicate.

Pharmacokinetic analysis of AK602 in hu-PBMC-NOG mice. Pharmacokinetic analysis of AK602 in hu-PBMC-NOG mice was performed as previously described (28). In brief, plasma samples were collected periodically over 12 h, following a single AK602 administration at a dose of 60 mg/kg of body weight dissolved in 400 μl of 4% hydroxypropyl-β cyclodextrin (HPBC). Each plasma sample (150 μl) was centrifuged at 3,000 rpm for 10 min, and the supernatant was vacuum concentrated and injected into the high-performance liquid chromatography (HPLC) system. The eluent was monitored at 255 nm of UV, and the AK602 concentration in plasma was determined.

Determination of amounts of AK602 persistently bound to CCR5 in hu-PBMC-NOG mice. Blood samples were collected from the tail vein of each hu-PBMC-NOG mouse at various time points following a single intraperitoneal administration of AK602 at a dose of 60 mg/kg. PBMC were isolated by density gradient centrifugation and stained with fluorescein isothiocyanate-conjugated monoclonal antibody 45531 (R&D Systems, Minneapolis, Minn.) specific for the C-terminal half of the second extracellular loop (ECL2B) of CCR5 (15) known to be competitively replaced by SDP derivatives (17) or with PE-conjugated monoclonal antibody 3A9, which binds to the N-terminus extracellular domain of CCR5 (17). PBMC were then subjected to FACS analysis.

Treatment of R5 HIV-1-infected hu-PBMC-NOG mice with anti-HIV-1 agents. Sixteen days after PBMC infusion, the mice were bled from the tail vein, and three-color flow cytometric analysis was performed to confirm positive engraftment of human HLA, CD4, and CD8 antigens on the cells recovered. HIV-$1_{JR\text{-}FL}$ (2,000 50% tissue culture infectious doses) was intraperitoneally inoculated to each mouse in which PBMC engraftment was confirmed. Twenty-four hours after the R5 HIV-1 inoculation, administration of AK602 (120 mg in 4% HPBC/kg/day, twice a day), ddI (50 mg in 4% HPBC/kg/day, twice a day), or saline was implemented and continued by day 16. On days 5 and 9 after the R5 HIV-1 inoculation, blood samples were collected from mouse tail veins for immunologic and virological monitoring (see below). On day 16, blood samples were collected by cardiocentesis, and the mice were sacrificed. The experimental protocol for the treatment is illustrated in Fig. 2.

Immunologic and virological monitoring. Human PBMC recovered from mice were subjected to immunologic and virological monitoring as previously described (23, 24). The $CD4^+/CD8^+$ cell ratios were determined by FACS analysis with PE-conjugated mouse anti-CD4 and peridinin chlorophyll protein-conjugated mouse anti-CD8 (BD Pharmingen) monoclonal antibodies. Determination of HIV-1 DNA copy numbers in recovered human PBMC was performed by real-time PCR assay with Taqman Master mixture (PE Biosystems) and HIV long terminal repeat-specific primers M667 (5′-GGC TAA CTA GGG AAC CCA CTG-3′) and AA55 (5′-CTG CTA GAG ATT TTC CAC ACT GAC-3′). HIV-1-specific products were quantified with the ABI 7700 detection system (Applied Biosystems, Foster City, Calif.), and cell numbers were determined with the RAG-1 gene. The numbers of $CD4^+$ cells were calculated based on the percentage of $CD4^+$ values obtained from the FACS analysis of each test PBMC sample, and R5 HIV-1 proviral DNA copy numbers were expressed as copy numbers per 10^5 $CD4^+$ cells. In some experiments, $CD4^+$ and $CD4^-$ cells were separated before real-time PCR assay with the rapid immunomagnetic CD4-positive cell isolation kit (Dynabeads M-450 CD4; Dynal Biotech, Inc., Lake

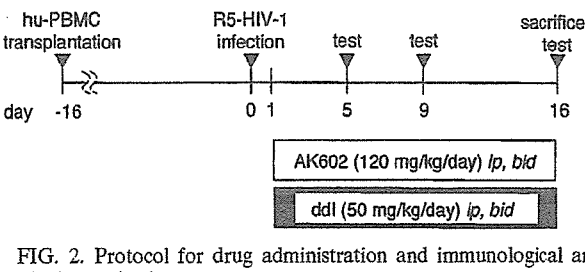

FIG. 2. Protocol for drug administration and immunological and virologic monitoring.

Success, N.Y.). The amounts of p24 antigen in murine sera were determined using a fully automated chemiluminescent enzyme immunoassay system (Lumipulse F; Fujirebio, Inc., Tokyo, Japan) as previously described (12). Plasma viral load was quantified with the AMPLICOR HIV-1 monitor test kit, version 1.5 (Roche Diagnostics, Branchburg, N.J.).

Statistical analyses. Nonparametric statistical analyses were performed by using the Mann-Whitney U test (Statview, version 5.0; Abacus Concepts, Berkeley, Calif.). The difference between viremia levels in two groups of mice was determined by the Wilcoxon rank sum test. For each mouse, the value of $\log_{10}$ RNA copies was calculated, and the slope corresponding to the rate of increase per day was determined by simple linear regression for the days (5, 9, and 16) of blood collection. The resulting slopes for all mice in the untreated groups were compared to the slopes of mice in each of the other two groups.

RESULTS

Transplanted PBMC in hu-PBMC-NOG mice are intensely activated and express high levels of CCR5. When we examined the proliferation profile of PBMC stimulated with PHA in vitro by treatment with the vital dye CFSE, which allows the analysis of cell proliferation as the CFSE's fluorescence intensity is halved per each cell division, there was only a slight shift to the left in the flow cytometric profile on days 1 and 2 of culture (Fig. 3A). On day 4 of culture, a discrete shift to the left was identified, suggesting that the PHA-PBMC underwent up to four cycles of proliferation in vitro by day 4. In contrast, PBMC transplanted and recovered on day 2 had apparently undergone ~4 cycles of proliferation; by day 4, a majority of cells had undergone up to 10 cycles and beyond in proliferation (Fig. 3B). It was possible that the CFSE-negative and weakly CFSE-positive cells which accumulated on days 2 and 4 (Fig. 3B) were murine cells that engulfed and degraded CFSE. We therefore conducted experiments in which the cells with CFSE dilution were directly confirmed to be human CCR5-positive cells. As can be seen in Fig. 3C, when cells were recovered from the spleen of an NOG mouse into which CFSE-labeled PBMC had been transplanted and stained with monoclonal antibody 45531, which is specific for the C-terminal half of the second extracellular loop (ECL2B) of CCR5 (15), the majority of such human $CCR5^+$ cells proved to be CFSE negative. We also examined the levels of cellular activation by the expression of HLA-DR on cell surface. The levels of HLA-DR expression in PBMC recovered from uninfected NOG mice 3 days after transplantation were much greater than those in 3-day-cultured PBMC following PHA stimulation (Fig. 3D). The fluorescence intensity in the same donor's PHA-PBMC examined on three different occasions was 21 ± 4, while that of the PBMC recovered from mice was 91 ± 25 (Fig. 3D). When we further assessed the levels of CCR5 expression, the PBMC recovered from the mice on day 3 proved to be strongly positive for CCR5 (Fig. 3E). The CCR5-positive fraction in the PBMC recovered was 49.7%, while that in PHA-PBMC was 27.3%. The mean fluorescence intensity of the $CCR5^+$ cell population was 141, compared to the $CCR5^+$ cell population in PHA-PBMC with a mean fluorescence intensity of 51. The estimated number of CCR5 expressed on the PBMC recovered on day 3 was 25,348 (as antibody binding sites per cell) while that on PHA-PBMC on day 3 in culture was 8,981 antibody binding sites as examined by quantitative FACS assay. These data indicate that the transplanted human PBMC were intensely activated and rapidly proliferating and expressed high levels of CCR5 on their cell surfaces.

Potent activity of AK602 against R5 HIV-1 in vitro. Among SDP derivatives we designed and synthesized, AK602 was identified to be highly potent against a broad spectrum of R5 HIV-1 strains, including MDR clinical R5 HIV-1 isolates in vitro with 50% inhibitory concentration (IC_{50}) values of 0.3 to 0.6 nM, although two previously published CCR5 antagonists (TAK779 and SCH-C) were substantially less potent than AK602 (Table 1). AK602 and other CCR5 antagonists failed to inhibit the replication of an X4 HIV-1 strain, HIV-1_{NL4-3}.

Pharmacokinetics of AK602 in hu-PBMC-NOG mice. We examined the pharmacokinetics of AK602 in hu-PBMC-NOG mice by intraperitoneally administering the compound at a dose of 60 mg/kg. Plasma samples were collected periodically up to 12 h and subjected to HPLC analysis. As shown in Fig. 4A, the concentration of AK602 reached the maximal concentration immediately after intraperitoneal administration and decreased rapidly. The calculated plasma half-life in the α-phase of the concentration curve was as short as 29 min.

AK602 persists on cell surface CCR5. As shown above, the plasma half-life of AK602 turned out to be short; however, considering that AK602 possesses such a high affinity to CCR5 and potent activity against R5 HIV-1 in vitro, it was thought possible that AK602 would remain attached on cellular CCR5 for an extensive period of time and exert anti-R5 HIV-1 activity even when the compound was depleted from circulation. To examine this possibility, we used two monoclonal antibodies, 45531 and 3A9. When human PBMC were recovered from a hu-PBMC-NOG mouse 2 and 6 h after AK602 administration (60 mg/kg) and stained with 45531, AK602 proved to block the binding of 45531 to CCR5 (Fig. 4B), while AK602 failed to block 3A9 binding to CCR5 (Fig. 4C), suggesting that AK602 did not elicit CCR5 internalization or shedding at all at least for 6 h. We subsequently examined whether AK602 remained on cellular CCR5 with the 45531 monoclonal antibody. When the cells were recovered from mice 2, 6, and 14 h after the AK602 administration, the mean values of the percentage of AK602 occupancy were 85 (four mice), 54 (three mice), and 16 (three mice), respectively. It was calculated that it took about 9 h for AK602 occupancy to be reduced by 50% (Fig. 4D).

Anti-R5 HIV-1 activity of AK602 persistently seen after its removal from culture medium. In another depletion experiment, we exposed $CCR5^+$ MAGI cells to AK602 for 30 min, depleted the compound from the culture by thorough washing, incubated the cells for various lengths of time, exposed the cells to HIV-1_{Ba-L}, further cultured the cells for 48 h, and determined whether HIV-1_{Ba-L} infection was blocked by AK602 exposure (Fig. 4E). When the $CCR5^+$ MAGI cells were exposed to 0.1 and 1 μM AK602 and exposed to HIV-1_{Ba-L} immediately afterward, the values for protection were 68 and 85%, respectively. When the cells were exposed to HIV-1_{Ba-L} 4 h after depletion, 49 and 72% of the cells were protected by 0.1 and 1 μM AK602. When the cells were exposed to HIV-1_{Ba-L} 12 and 24 h after depletion, 57 and 45% of the cells were seen protected by 1 μM, respectively (Fig. 4E).

Effects of AK602 on $CD4^+$ and $CD8^+$ cell counts in R5 HIV-1-infected hu-PBMC-NOG mice. PBMC were recovered from murine blood samples collected on days 5, 9, and 16 after R5 HIV-1 inoculation and subjected to flow cytometric analysis for determination of $CD4^+/CD8^+$ cell ratios. As shown in Fig. 5A, in PBMC recovered on day 16 from a representative

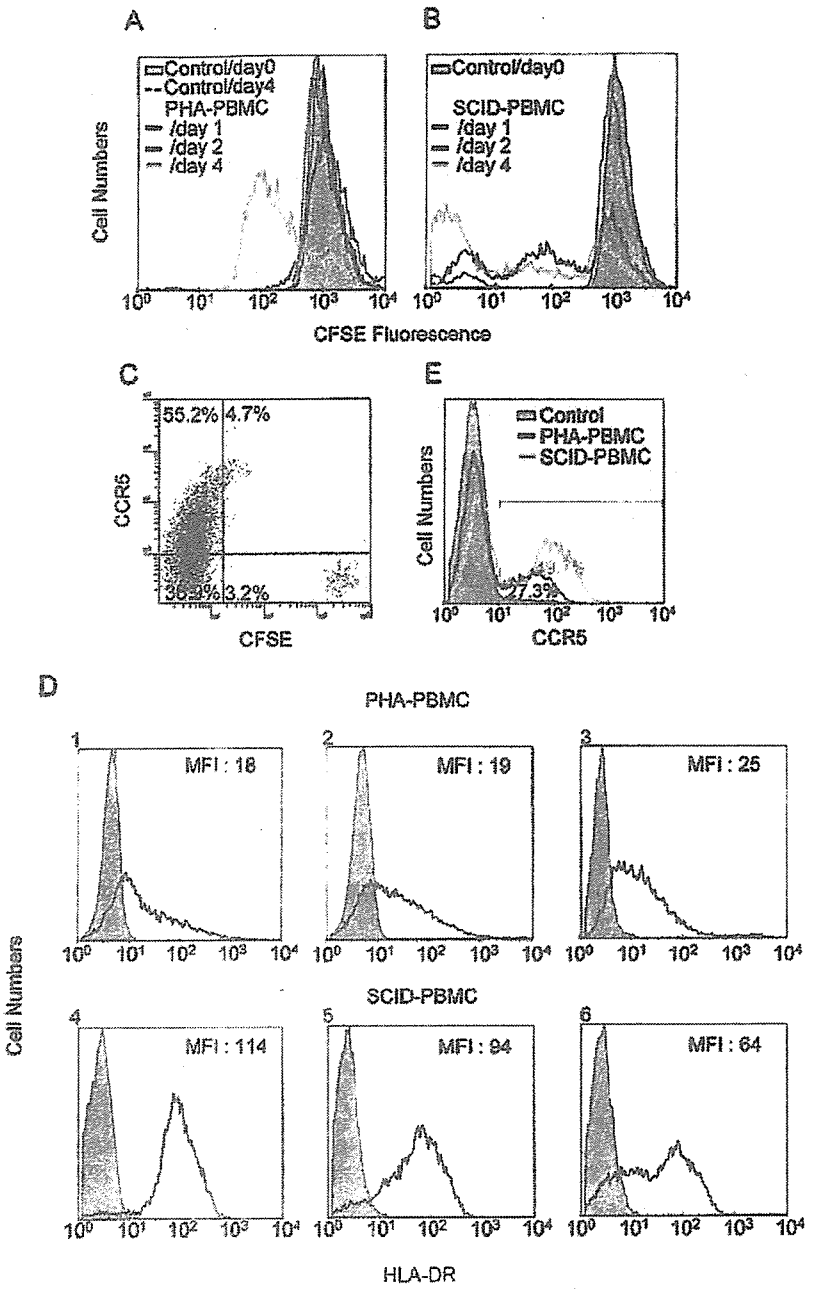

FIG. 3. Transplanted PBMC are intensely activated and express high levels of CCR5. (A and B) Proliferation profiles of PHA-PBMC and transplanted and recovered PBMC. Freshly prepared PBMC were incubated with the vital dye CFSE, and one part of such PBMC preparation was stimulated with PHA, while the other part was intraperitoneally transplanted to mice. On days 1, 2, and 4, the cells were harvested and the fluorescence intensity of CFSE was determined. Note that transplanted PBMC recovered on day 2 had undergone ~4 cycles of proliferation; by day 4, a majority of cells had undergone ~10 cycles and more of proliferation. (C) CCR5 expression level and CFSE intensity in human PBMC harvested from a spleen of hu-PBMC-NOG mouse on day 4. (D) Intense activation of PBMC after transplantation. PBMC stimulated with PHA and cultured for 4 days (panels 1 to 3) and transplanted PBMC recovered from the uninfected mice on day 4 (panels 4 to 6) were stained with an anti-HLA-DR monoclonal antibody. Note that HLA-DR expression levels in transplanted PBMC were much higher than those in PHA-PBMC. (E) CCR5 expression profiles of PHA-PBMC and transplanted PBMC. PBMC stimulated with PHA and cultured for 3 days and transplanted PBMC recovered from the uninfected mice on day 3 were stained with PE-conjugated anti-CCR5 monoclonal antibody 3A9 and subjected to flow cytometric analysis. SCID-PBMC, PBMC transplanted and recovered.

R5 HIV-1-infected, saline-treated mouse, there were only few $CD4^+$ cells (3.9% [1.4% + 2.5%]) resulting in a $CD4^+/CD8^+$ cell ratio of 0.05. However, a distinct $CD4^+$ cell population (55.1% [4.4% + 50.7%]) resulting in a $CD4^+/CD8^+$ ratio of 1.84 (Fig. 5B) was seen in PBMC recovered from an AK602-treated mouse, and the size of this $CD4^+$ cell population was comparable to that seen in a ddI-treated mouse (53.2% [3.8% + 49.4%]) and that in an uninfected mouse (48.9% [3.8% +

TABLE 1. Anti HIV-1 activity of novel SDP derivatives in PBMC[a]

Compound	IC_{50} value in p24 assay (nM)					
	HIV-1_{Ba-L} (R5)	HIV-1_{JRFL} (R5)	HIV-1_{MOKW} (R5)	HIV-1_{MM} ($R5_{MDR}$)	HIV-1_{ISL} ($R5_{MDR}$)	HIV-1_{NL4-3} (X4)
AK602	0.5 ± 0.3	0.2 ± 0.1	0.3 ± 0.2	0.7 ± 0.3	0.4 ± 0.2	>1,000
TAK779	14 ± 5	6 ± 2	9 ± 3	12 ± 4	10 ± 3	>1,000
SCH-C	3 ± 2	2 ± 1	2 ± 1.5	2.5 ± 1	2 ± 1	>1,000
ZDV	13 ± 5	7 ± 3	10 ± 6	520 ± 75	64 ± 13	9 ± 5
SQV	8 ± 3	6 ± 2	6 ± 3	212 ± 56	276 ± 44	10 ± 4

[a] IC_{50}s were determined by using PHA-PBMC isolated from three different donors, and the inhibition of p24 Gag protein production was used as an endpoint. All assays were conducted in triplicate. The results shown represent arithmetic means (±1 standard deviation) of three independently conducted assays. HIV-1_{MOKW} was isolated from a drug-naive AIDS patient, and HIV-1_{ISL} and HIV-1_{MM} were isolated from patients who received antiretroviral therapy for a long period of time and whose virus loads showed a number of RT and PR mutations. Two previously published CCR5 inhibitors, TAK779 and SCH-C, and zidovudine (ZDV) and saquinavar (SQV) were used as reference compounds.

45.1%]), resulting in the ratios of 1.43 and 1.40 (Fig. 5C and D), respectively. Figure 6A illustrates the overall profiles of $CD4^+/CD8^+$ cells ratios on day 16 in the four groups. The mean $CD4^+/CD8^+$ cell ratio in mice (n = 7) given saline was 0.1 (range, 0.06 to 0.20). In contrast, the ratios in AK602-treated mice (n = 8) were significantly higher with a mean value of 0.92 (range, 0.23 to 1.89; P = 0.001), which was comparable to that in ddI-treated mice (n = 9; mean, 1.29; range, 0.38 to 2.68; P = 0.001) and uninfected mice (n = 7; mean, 1.0; range, 0.50 to 1.49). The numbers of $CD4^+$ cells/μl

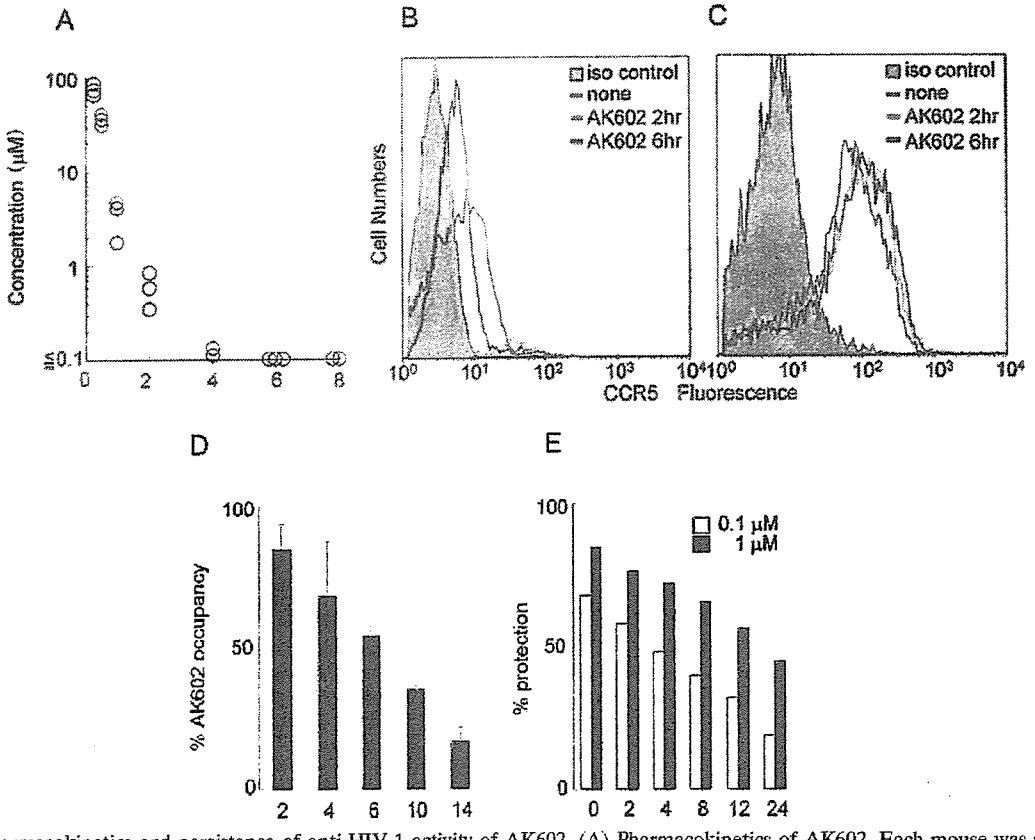

FIG. 4. Pharmacokinetics and persistence of anti-HIV-1 activity of AK602. (A) Pharmacokinetics of AK602. Each mouse was administered AK602 at a dose of 60 mg/kg, and blood samples were taken at 15, 30, 60, 120, 240, 480, and 720 min. Plasma concentrations of AK602 determined by HPLC analysis at 15, 30, 60, 120, and 240 min were 76.2, 36.1, 3.5, 0.6, and 0.13 μM, respectively. AK602 was not detected at later time points. (B and C) No CCR5 internalization or shedding was caused by AK602. Human PBMC were recovered 2 and 6 h after AK602 administration and stained with 45531 (B) or 3A9 (C). (D) Sustained AK602 occupancy on cell surfaces. At indicated periods of time after a bolus of AK-602 (60 mg/kg) was administered to hu-PBMC-NOG mice, PBMC were recovered and the percentages of AK602 occupancy on cellular CCR5 were determined with fluorescein isothiocyanate-conjugated monoclonal antibody 45531. (E) Persistence of in vitro activity of AK602 against R5 HIV-1 after AK602 depletion. $CCR5^+$ MAGI cells were exposed to 0.1 or 1 μM AK602 for 30 min and thoroughly washed to deplete AK602 from the medium. The cells were subsequently cultured for the indicated periods of time, exposed to HIV-1_{Ba-L}, and further cultured for 48 h, when the cells were harvested and lysed with Triton X-100-containing PBS. A solution containing chlorophenol red-β-D-galactopyranoside was added, the optical density was measured, and the percentage of protection was determined.

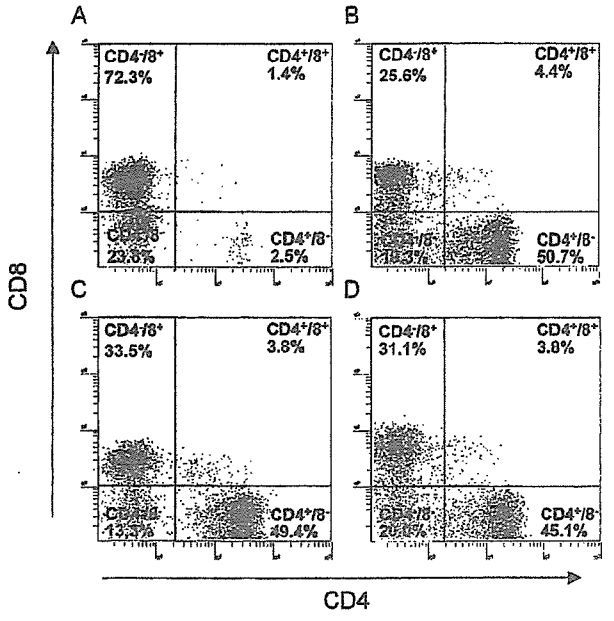

FIG. 5. Effects of AK602 on $CD4^+$ and $CD8^+$ cell counts in infected hu-PBMC-NOG mice. PBMC recovered on day 16 after R5 HIV-1 inoculation were subjected to flow cytometry. Shown are representative flow cytometric analysis profiles. Note that only 3.9% of $CD4^+$ cells were seen (A), resulting in a $CD4^+/CD8^+$ cell ratio of 0.05 in a mouse given saline, while distinct numbers of $CD4^+$ cells (55.1 and 53.2%) (B and C) were seen in AK602- and ddI-administered infected mice, resulting in $CD4^+/CD8^+$ cell ratios of 1.84 and 1.43, respectively. In an uninfected mouse (D), 48.9% of cells were positive for CD4, with a $CD4^+/CD8^+$ cell ratio of 1.40.

in saline-treated mice were significantly less than those of AK602-treated, ddI-treated, or uninfected mice (Fig. 6B).

Effects of AK602 on R5 HIV-1 proviral DNA copy numbers and serum p24 levels in R5 HIV-1-infected hu-PBMC-NOG mice. We next asked which population harbored proviral DNA in the cells recovered from R5 HIV-1-infected hu-PBMC-NOG mice, by purifying $CD4^+$ and $CD4^-$ cell populations and determining proviral DNA copy numbers in each population. As shown in Table 2, more than 99% of proviral DNA was found in $CD4^+$ cells and <0.3% of proviral DNA was detected in $CD4^-$ cells derived from saline-treated mice, indicating that R5 HIV-1 infection occurred in $CD4^+$ cells in the hu-PBMC-transplanted NOG environment. As illustrated in Fig. 6C, the mean number of R5 HIV-1 proviral DNA copies was 2.0×10^5 (range, 2.6×10^4 to 1.7×10^6) per 10^5 $CD4^+$ cells in R5 HIV-1-infected mice ($n = 7$) given saline. However, values for mice in groups given AK602 and ddI were 1.3×10^3 (range, 2.3×10^2 to 7.9×10^3; $P = 0.001$) and 1.8×10^2 (range, $<10^2$ to 7.9×10^2; $P = 0.001$), respectively.

The amounts of R5 HIV-1 p24 in serum were also found to be very high in saline-treated mice, with a mean amount of 1.1×10^5 pg/ml (range, 3.1×10^4 to 2.8×10^5 pg/ml). AK602 and ddI were found to significantly suppress the serum p24 amounts as examined on day 16 with a mean amount of 5.6×10^3 pg/ml (range, 8.1×10^2 to 2.1×10^4 pg/ml; $P = 0.001$) and 7.1×10^2 pg/ml (range, 1.3×10^2 to 1.1×10^4 pg/ml; $P = 0.001$), respectively (Fig. 6D).

AK602 suppressed R5 HIV-1 viremia in hu-PBMC-NOG mice. As described above, the PBMC transplanted to NOG mice were intensely activated in the xenogeneic environment and had undergone ~4 cycles of proliferation by day 2; a majority of the cells had undergone ≥10 cycles of proliferation by day 4 (Fig. 3B). These data suggested that R5 HIV-1 might extensively replicate in the hu-PBMC-NOG mice immediately after R5 HIV-1 inoculation. When we collected blood samples on days 5, 9, and 16 following the inoculation and determined R5 HIV-1 RNA copy numbers in infected, saline-treated mice ($n = 7$), the geometric mean copy number was 8.6×10^3/ml (range, 1.7×10^3 to 1.0×10^5) on day 5 and rapidly increased to 1.9×10^5/ml (range, 2.2×10^4 to 3.0×10^6) on day 9; by day 16, the mean copy number had reached 7.7×10^5/ml (range, 2.6×10^5 to 3.0×10^6/ml). However, AK602 significantly suppressed viremia by ~1.1 log, as examined on day 5; the mean numbers of R5 HIV-1 RNA copies in AK602-administered mice were 1.6 and 1.8 logs lower than those in saline-treated mice examined on days 9 and 16, respectively (Fig. 7). Comparable viremia suppression was seen in the mice receiving ddI (Fig. 7). It was noted that although AK602 did not completely prevent the viremia from further increasing after day 5, there was a clear reduction in the viremia increase rates. The mean slopes (change in RNA copies per day over the range of data from 5 to 16 days) for the group receiving saline was 0.167 ± 0.042, whereas those for the AK602 and ddI groups were 0.102 ± 0.041 and 0.091 ± 0.037, respectively. Thus, the rates of increase in the AK602 ($P = 0.0057$) and ddI ($P = 0.0023$) mice were significantly lower than that for the mice given saline, indicating that both of the agents significantly inhibited R5 HIV-1 replication in this mouse model over the range of days evaluated. No apparent AK602- or ddI-associated adverse effects were seen throughout the study period.

DISCUSSION

In the present hu-PBMC-NOG mouse model, human $CD4^+/CD8^+$ cell ratios went down to 0.1 by 16 days after R5 HIV-1 inoculation, the amounts of proviral DNA and p24 gag antigen reached 10^5 to 10^6 copies/10^5 $CD4^+$ cells and 10^5 pg/ml, respectively (Fig. 6), and no mice failed to be infected with R5 HIV-1. It is noteworthy that the use of NOG mice provides a higher engraftment rate than with other SCID mice such as NOD/Shi-SCID mice treated with anti-NK cell antibody or the β_2-microglobulin-deficient NOD-SCID mice (10). With NOG mice, the chimeric rate of 30 to 40% is achieved, and cord blood $CD34^+$ cells have been shown to "take" with as few as 100 cells (10). Moreover, all infected mice developed high levels of R5 HIV-1 viremia by day 16, reaching as high as 10^6 copies/ml (Fig. 7). It is worth noting that the notably high levels of HIV-1 viremia seen in the present mouse model by 16 days after R5 HIV-1 exposure can be seen only on acute infection or up to 10 years after HIV infection in humans (3, 4).

In the present study, we found that the conspicuous susceptibility to the infectivity and replication of R5 HIV-1 in these mice appeared to stem from the hyperactivation of the implanted human PBMC. The implanted PBMC were highly activated in the xenogeneic environment, expressed quite high

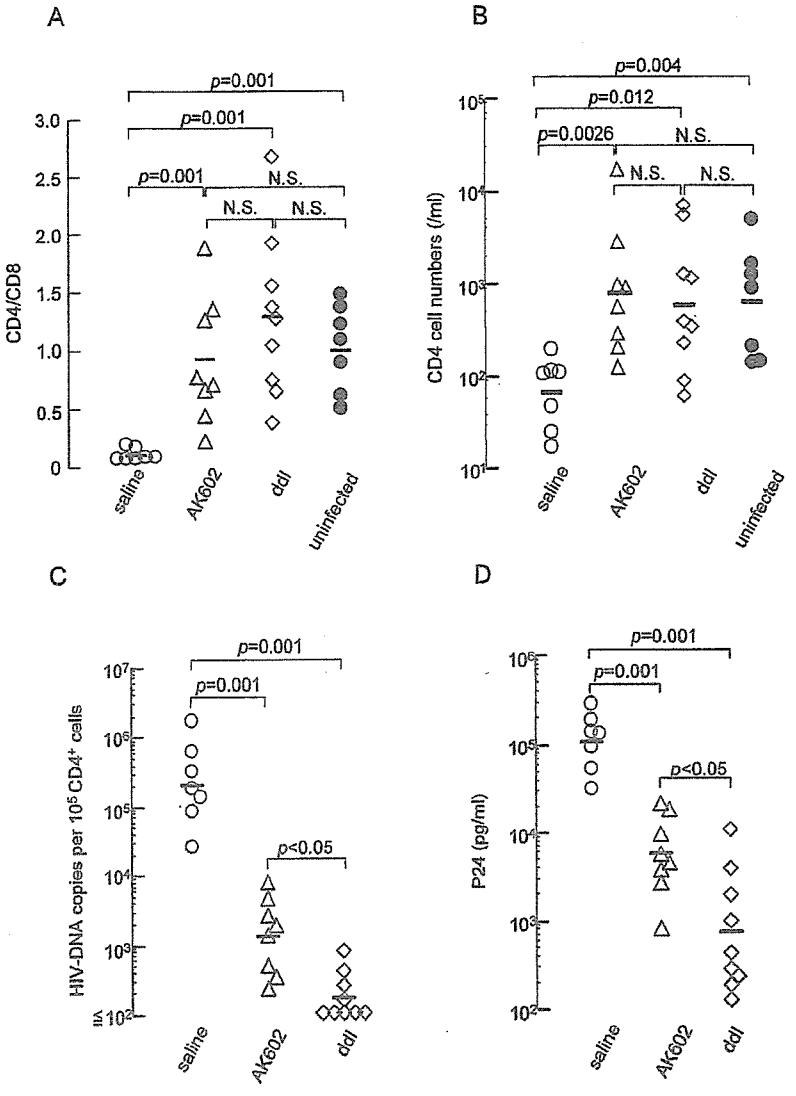

FIG. 6. Effects of AK602 on $CD4^+/CD8^+$ ratios and the amounts of proviral DNA and HIV-1 p24 in infected hu-PBMC-NOG mice. (A) Overall profiles of $CD4^+/CD8^+$ cell ratios. Note that the mean $CD4^+/CD8^+$ cell ratio in mice given saline ($n = 7$) was 0.1, while those in mice given AK602 or ddI were 0.92 and 1.29, respectively. The mean ratio in uninfected mice was 1.0. (B) Numbers of $CD4^+$ cells per microliter in each mouse group. (C) HIV-1 proviral DNA copy numbers in $CD4^+$ cells from each mouse group were determined by real-time PCR assay. Values are shown per 10^5 $CD4^+$ cells, as described in Materials and Methods. Note that the mean number of HIV-1 proviral DNA copies was 2.0×10^5 per 10^5 $CD4^+$ cells in mice given saline, while those in AK602- and ddI-treated groups were 1.3×10^3 and 1.8×10^2 per 10^5 $CD4^+$ cells (both, $P = 0.001$), respectively. (D) Amounts of plasma p24 antigen. Note that the amounts of p24 in plasma were high in saline-treated mice while AK602 and ddI significantly suppressed the serum p24 amounts as examined on day 16 after $HIV\text{-}1_{Ba\text{-}L}$ inoculation. The short bars indicate the arithmetic (A) and geometric (B, C, and D) means obtained.

levels of HLA-DR, and rapidly and continuously proliferated immediately after intraperitoneal infusion (Fig. 3A, B, and D). Moreover, the implanted PBMC expressed as much as 2.8-fold-higher levels of CCR5 on day 3 following implantation compared to PHA-PBMC on day 3 in culture (Fig. 3E). The combination of rapid proliferation and high levels of CCR5 expression of the implanted PBMC should explain the reason R5 HIV-1 rapidly replicated in the hu-PBMC-NOG mice and presented such high levels of R5 HIV-1 viremia. In this regard, only a few groups to date have documented the levels of viremia in the scientific literature. Among them are those by Garaci et al. (8) and Koyanagi et al. (14). The former documented high levels of viremia with a peak of 2.67×10^6 copies/ml in hu-PBL-NOD-SCID mice in which HIV-1-infected macrophages were inoculated, unlike our NOG mouse model where HIV-1 was directly inoculated. The latter report by Koyanagi et al. does not have viremia data but has data on p24 levels with a geometric mean of 11,092 pg/ml on day 14 after HIV-1 inoculation. However, the variation was much greater (178 to 1,434,444 pg/ml). Thus, one can say that the present model provides a greater reproducibility of high viremia levels than the mouse system reported by Koyanagi (14). It should be noted that the high levels of viremia and high engraftment rate achieved in this mouse model made it possible to monitor the

TABLE 2. Comparison of HIV-1 proviral DNA in human $CD4^+$ and $CD4^-$ cell fractions[a]

Sample	HIV-1 DNA copies (10^5 cells)		
	SCID-PBMC	$CD4^+$ cells	$CD4^-$ cells
Saline 1	138,858	162,193	461
Saline 2	135,967	117,949	<100
Saline 3	83,863	94,590	<100
AK602 1	3,390	2,300	<100
AK602 2	5,575	4,606	<100
AK602 3	1,925	1,398	<100
ddI 1	301	516	<100
ddI 2	793	1,317	<100
ddI 3	<100	118	<100

[a] HIV-1 proviral DNA copy numbers were determined by real-time PCR assay of unseparated human PBMC and purified $CD4^+$ and $CD4^-$ cells, following recovery from hu-PBMC-NOG mice. Values are shown per 10^5 cells, as described in Materials and Methods.

changes in the viremia levels periodically in the same set of mice without sacrificing them, while most of the previously described SCID mouse models required mice to be sacrificed at each time point of testing (25, 29, 30) or needed further in vitro coculture of the PBMC recovered from the mice with freshly prepared uninfected target cells for an additional period of days (9, 34).

We demonstrated in this study that a novel SDP derivative, AK602, exerted highly potent activity against laboratory and primary R5 HIV-1 strains as well as MDR R5 HIV-1 variant with IC_{50} values of subnanomolar concentrations (Table 1). It should be noted that AK602 represents a novel SDP derivative, which binds to human CCR5 but not to human CXCR4, CCR1, CCR2, CCR3, CCR4 or murine CCR5; blocks the binding of MIP-1α to CCR5 with an extremely high affinity (K_d values of ~3 nM); potently blocks HIV-1-gp120/CCR5 binding; and exerts potent activity against a wide spectrum of laboratory and primary R5 HIV-1 isolates including MDR HIV-1 and HIV-1 strains of various clades with IC_{50} values of 0.2 to 0.6 nM in vitro (K. Maeda, H. Ogata, S. Harada, Y. Tojo, T. Miyakawa, H. Nakata, Y. Takaoka, S. Shibayama, D. Fukushima, J. Moravek, E. Arnold, and H. Mitsuya, 11th Conf. Retrovir. Opp. Infect., abstr. 540, 2004; J. Demarest et al., XV Int. AIDS Conf., abstr. WeOrA1231, 2004). The plasma half-life of AK602 in the hu-PBMC-NOG mice, however, proved to be as short as 29 min when the agent was administered intraperitoneally (Fig. 4A). Considering that AK602 possesses such a high binding affinity to CCR5, we presumed that AK602 could remain on CCR5 for an extended period of time even after the agent was removed from the bloodstream in mice. The high and extensive level of AK602 occupancy observed in PBMC recovered from mice receiving AK602 substantiated this presumption (Fig. 4D). The subsequent in vitro experiment in which $CCR5^+$ MAGI cells were incubated with AK602 but exposed to R5 HIV-1 after the removal of the compound from the culture medium showed that AK602's anti-R5 HIV-1 activity can persist for an extensive period of time even if AK602 is no longer present in the culture (Fig. 4E). It is of note that unlike certain reports of in vivo anti-HIV-1 activity of chemokine antagonists which were administered before HIV-1 inoculation, thus demonstrating prophylactic effects of such agents (9, 30), the present system demonstrates anti-HIV-1 treatment after the establishment of HIV-1 infection, analogous to antiviral therapy in clinical settings.

When highly active antiretroviral therapy exerts its potent antiviral effects in clinical settings, a decrease in HIV-1 viremia is seen often within weeks, ultimately resulting in undetectable viremia; however in the present study, the viremia levels in mice receiving AK602 or ddI continued to increase although the rate of increment significantly declined (Fig. 7). The failure of AK602 and ddI to decrease viremia levels could be due in part to such a rapid viral replication in hyperactivated and proliferating $CD4^+$ cells. As discussed earlier, PBMC recovered from the hu-PBMC-NOG mice were highly positive for CCR5 and HLA-DR (Fig. 3D and E), compared to the levels of activation seen in the same donor's PHA-PBMC. It should be noted, however, that the mean numbers of proviral DNA copies on day 16 in mice receiving AK602 and ddI were 1.3×10^3 and 1.8×10^2 per 10^5 $CD4^+$ cells, respectively (Fig. 6C), suggesting that most $CD4^+$ cells (98.7 and 99.8% on average, respectively) were free of HIV-1 and proliferating in those

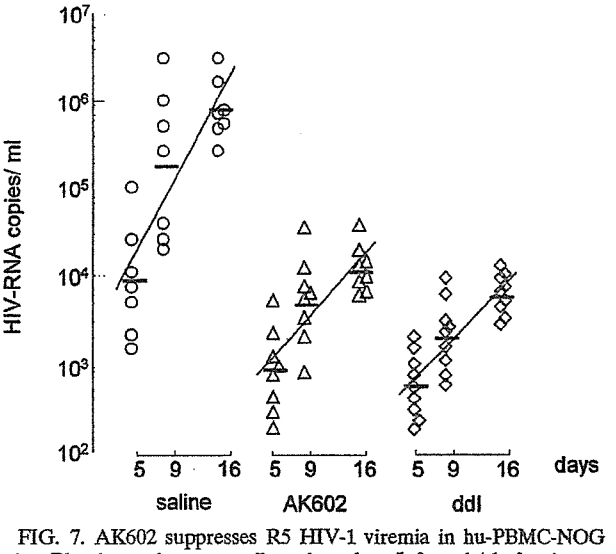

FIG. 7. AK602 suppresses R5 HIV-1 viremia in hu-PBMC-NOG mice. Blood samples were collected on days 5, 9, and 16 after inoculation and were subjected to the determination of R5 HIV-1 RNA copy numbers. Note that the copy numbers in saline-treated mice rapidly increased and reached ~10^6/ml by day 16, while AK602 significantly suppressed the viremia by 1.6 and 1.8 logs as examined on day 9 ($P = 0.001$ compared to saline-treated mice) and day 16 ($P = 0.001$), respectively. Comparable viremia suppression was seen in ddI-treated mice, except on day 16, when ddI activity was greater than that of AK602 ($P = 0.027$). Note that there was a clear reduction in the rate of increase of viremia as well. When the values of $\log_{10}$ HIV-1 RNA copies were calculated and the slopes corresponding to the rates of increase per day were determined, the resulting mean slope (solid line) for the saline-treated mice was 0.167 ± 0.042, whereas those for the AK602- and ddI-treated mice were 0.102 ± 0.041 and 0.091 ± 0.037, respectively. The increase rate for saline-treated mice was significantly higher than those of AK602-treated mice ($P = 0.0057$) and ddI-treated mice ($P = 0.0023$), respectively. The horizontal bars and solid lines represent the geometric means of HIV-1 RNA copy numbers and the slopes calculated, respectively.

mice on day 16 after the virus inoculation, if one copy of proviral DNA was postulated to reside in one $CD4^+$ cell.

One of us (Y.K.) previously attempted to investigate the mechanism of $CD4^+$ cell depletion seen in individuals with HIV-1 infection by employing a PBMC-transplanted NOD (NOD/Shi) *scid/scid* mouse system (24). Massive apoptosis was observed in HIV-1-uninfected $CD4^+$ cells in the spleens of the HIV-1-infected NOD-*scid/scid* mice. A combination of terminal deoxynucleotidyl transferase-mediated dUTP nick-end labeling and immunostaining for death-inducing tumor necrosis factor (TNF) family molecules showed that apoptotic cells were frequently found in conjugation with TNF-related apoptosis-inducing ligand (TRAIL)-expressing $CD3^+$ $CD4^+$ human T cells. Further observation that a neutralizing anti-TRAIL antibody inhibited the development of $CD4^+$ cell apoptosis suggested that a large number of HIV-1-uninfected $CD4^+$ cells undergo TRAIL-mediated apoptosis, contributing to the marked depletion of $CD4^+$ cells (24). The observation by Miura and his colleagues that the number of TRAIL-positive cells was consistently higher in HIV-1-infected mice than in uninfected ones makes it apparent that TRAIL expression is induced upon HIV-1 infection (23, 24). In this regard, the present observation that AK602 and ddI potently blocked the decrease in $CD4^+$ cells in spite of the rather increasing HIV-1 viremia in the face of AK602 or ddI (Fig. 7) suggests that the mere presence of viremia might not be sufficient for the HIV-induced apoptosis in $CD4^+$ cells. Our observation that most surviving $CD4^+$ cells in mice receiving AK602 or ddI were free of HIV-1 (see above) suggests that these anti-HIV-1 agents might block not only de novo HIV-1 infection, but also bystander killing of uninfected $CD4^+$ cells. The present data also suggest that a certain factor(s) such as cytokines produced by the freshly HIV-1-infected cells might mediate the apoptosis of bystander $CD4^+$ cells through the upregulation of TRAIL expression, death receptors (e.g., DR4 and DR5), and/or downregulation of decoy receptors (e.g., DcR1 and DcR2) (26, 27). However, experiments with a combination of terminal deoxynucleotidyl transferase-mediated dUTP nick-end labeling and TNF family molecules have to be conducted for better understanding of the bystander killing in regard to AK602's effects.

It is of note that several CCR5 antagonists are currently in various stages of development. AK602 has recently been administered to healthy adult subjects in a phase I clinical trial and shown to bind to CCR5 for an extended period of time, suggesting that an oral formulation with fewer administrations and lower dosage is possible for AK602 as a therapeutic agent for HIV-1 infection (J. Demarest, K. Adkison, S. Sparks, A. Shachoy-Clark, K. Schell, S. Reddy, L. Fang, K. O'Mara, S. Shibayama, and S. Piscitelli, 11th Conf. Retrovir. Opp. Infect., abstr. 139, 2004). Taken together, our observations that plasma viral load reached $\sim 10^6$ RNA copies/ml and that AK602 potently inhibited the replication of R5 HIV-1 strongly suggest that the present hu-PBMC-NOG mouse AIDS model could serve as a useful instrument for analyzing the pathogenesis of HIV-1 infection and testing the efficacy of antiviral agents.

ACKNOWLEDGMENTS

We thank Seth Steinberg for statistical analysis and Naoko Misawa, Yuji Kawano, and Hiromi Ogata for technical assistance and discussion.

This work was supported in part by grant-in-aids for Scientific Research on Priority Areas (14207025 and 15019086) from the Japanese Ministry of Education, Science, Sports, Culture and Technology of Japan (Monbu-Kagakusho) and a grant for AIDS Research (H15-AIDS-001) from the Ministry of Health, Labor, and Welfare of Japan (Kosei-Rohdosho).

REFERENCES

1. **Baba, M., O. Nishimura, N. Kanzaki, M. Okamoto, H. Sawada, Y. Iizawa, M. Shiraishi, Y. Aramaki, K. Okonogi, Y. Ogawa, K. Meguro, and M. Fujino.** 1999. A small-molecule, nonpeptide CCR5 antagonist with highly potent and selective anti HIV-1 activity. Proc. Natl. Acad. Sci. USA **96**:5698–5703.
2. **Carr, A., K. Samaras, A. Thorisdottir, G. R. Kaufmann, D. J. Chisholm, and D. A. Cooper.** 1999. Diagnosis, prediction, and natural course of HIV-1 protease-inhibitor associated lipodystrophy, hyperlipidaemia, and diabetes mellitus: a cohort study. Lancet **353**:2093–2099.
3. **Dean, M., M. Carrington, C. Winkler, G. A. Huttley, M. W. Smith, R. Allikmets, J. J. Goedert, S. P. Buchbinder, E. Vittinghoff, E. Gomperts, S. Donfield, D. Vlahov, R. Kaslow, A. Saah, C. Rinaldo, R. Detels, and S. J. O'Brien.** 1996. Genetic restriction of HIV-1 infection and progression to AIDS by a deletion allele of the CKR5 structural gene. Hemophilia Growth and Development Study, Multicenter AIDS Cohort Study, Multicenter Hemophilia Cohort Study, San Francisco City Cohort, ALIVE Study. Science **273**:1856–1862.
4. **Easterbrook, P. J.** 1999. Long-term non-progression in HIV infection: definitions and epidemiological issues. J. Infect. **38**:71–73.
5. **Fauci, A. S.** 1999. The AIDS epidemic—considerations for the 21st century. N. Engl. J. Med. **341**:1046–1050.
6. **Finzi, D., J. Blankson, J. D. Siliciano, J. B. Margolick, K. Chadwick, T. Pierson, K. Smith, J. Lisziewicz, F. Lori, C. Flexner, T. C. Quinn, R. E. Chaisson, E. Rosenberg, B. Walker, S. Gange, J. Gallant, and R. F. Siliciano.** 1999. Latent infection of CD4+ T cells provides a mechanism for lifelong persistence of HIV-1, even in patients on effective combination therapy. Nat. Med. **5**:512–517.
7. **Gartner, S., P. Markovits, D. M. Markovitz, M. H. Kaplan, R. C. Gallo, and M. Popovic.** 1986. The role of mononuclear phagocytes in HTLV-III/LAV infection. Science **233**:215–219.
8. **Garaci, E., S. Aquaro, C. Lapenta, A. Amendola, M. Spada, S. Covaceuszach, C. F. Perno, and F. Belardelli.** 2003. Anti-nerve growth factor Ab abrogates macrophage-mediated HIV-1 infection and depletion of CD4+ T lymphocytes in hu-SCID mice. Proc. Natl. Acad. Sci. USA **100**:8927–8932.
9. **Ichiyama, K., S. Yokoyama-Kumakura, Y. Tanaka, R. Tanaka, K. Hirose, K. Bannai, T. Edamatsu, M. Yanaka, Y. Niitani, N. Miyano-Kurosaki, H. Takaku, Y. Koyanagi, and N. Yamamoto.** 2003. A duodenally absorbable CXC chemokine receptor 4 antagonist, KRH-1636, exhibits a potent and selective anti-HIV-1 activity. Proc. Natl. Acad. Sci. USA **100**:4185–4190.
10. **Ito, M., H. Hiramatsu, K. Kobayashi, K. Suzue, M. Kawahata, K. Hioki, Y. Ueyama, Y. Koyanagi, K. Sugamura, K. Tsuji, T. Heike, and T. Nakahata.** 2002. NOD/SCID/γ(c)(null) mouse: an excellent recipient mouse model for engraftment of human cells. Blood **100**:3175–3182.
11. **Kavlick, M. F., and H. Mitsuya.** 2001. The emergence of drug resistant HIV-1 variants and its impact on antiretroviral therapy of HIV-1 infection, p. 279–312. *In* E. De Clercq (ed.), The art of antiretroviral therapy. American Society for Microbiology, Washington, D.C.
12. **Koh, Y., H. Nakata, K. Maeda, H. Ogata, G. Bilcer, T. Devasamudram, J. F. Kincaid, P. Boross, Y. F. Wang, Y. Tie, P. Volarath, L. Gaddis, R. W. Harrison, I. T. Weber, A. K. Ghosh, and H. Mitsuya.** 2003. Novel bis-tetrahydrofuranylurethane-containing nonpeptidic protease inhibitor (PI) UIC-94017 (TMC114) with potent activity against multi-PI-resistant human immunodeficiency virus in vitro. Antimicrob. Agents Chemother. **47**:3123–3129.
13. **Koyanagi, Y., S. Miles, R. T. Mitsuyasu, J. E. Merrill, H. V. Vinters, and I. S. Chen.** 1987. Dual infection of the central nervous system by AIDS viruses with distinct cellular tropisms. Science **236**:819–822.
14. **Koyanagi, Y., Y. Tanaka, J. Kira, M. Ito, K. Hioki, N. Misawa, Y. Kawano, K. Yamasaki, R. Tanaka, Y. Suzuki, Y. Ueyama, E. Terada, T. Tanaka, M. Miyasaka, T. Kobayashi, Y. Kumazawa, and N. Yamamoto.** 1997. Primary human immunodeficiency virus type 1 viremia and central nervous system invasion in a novel hu-PBL-immunodeficient mouse strain. J. Virol. **71**:2417–2424.
15. **Lee, B., M. Sharron, L. J. Montaner, D. Weissman, and R. W. Doms.** 1999. Quantification of CD4, CCR5, and CXCR4 levels on lymphocyte subsets, dendritic cells, and differentially conditioned monocyte-derived macrophages. Proc. Natl. Acad. Sci. USA **96**:5215–5220.
16. **Lyons, A. B.** 2000. Analysing cell division in vivo and in vitro using flow cytometric measurement of CFSE dye dilution. J. Immunol. Methods **243**: 147–154.
17. **Maeda, K., K. Yoshimura, S. Shibayama, H. Habashita, H. Tada, K. Sagawa, T. Miyakawa, M. Aoki, D. Fukushima, and H. Mitsuya.** 2001. Novel low molecular weight spirodiketopiperazine derivatives potently inhibit R5

HIV-1 infection through their antagonistic effects on CCR5. J. Biol. Chem. **276**:35194–35200.
18. **Maeda, Y., M. Foda, S. Matsushita, and S. Harada.** 2000. Involvement of both the V2 and V3 regions of the CCR5-tropic human immunodeficiency virus type 1 envelope in reduced sensitivity to macrophage inflammatory protein 1α. J. Virol. **74**:1787–1793.
19. **McCune, J. M., R. Namikawa, C. C. Shih, L. Rabin, and H. Kaneshima.** 1990. Suppression of HIV infection in AZT-treated SCID-hu mice. Science **247**:564–566.
20. **Mitsuya, H., and S. Broder.** 1986. Inhibition of the in vitro infectivity and cytopathic effect of human T-lymphotropic virus type III/lymphadenopathy virus-associated virus (HTLV-III/LAV) by 2′,3′-dideoxynucleosides. Proc. Natl. Acad. Sci. USA **83**:1911–1915.
21. **Mitsuya, H., and S. Broder.** 1987. Strategies for antiviral therapy in AIDS. Nature **325**:773–778.
22. **Mitsuya, H., and J. Erickson.** 1999. Discovery and development of antiretroviral therapeutics for HIV infection, p. 751–780. *In* T. C. Merigan, J. G. Bartlet, and D. Bolognesi (ed.), Textbook of AIDS medicine. Williams & Wilkins, Baltimore, Md.
23. **Miura, Y., N. Misawa, Y. Kawano, H. Okada, Y. Inagaki, N. Yamamoto, M. Ito, H. Yagita, K. Okumura, H. Mizusawa, and Y. Koyanagi.** 2003. Tumor necrosis factor-related apoptosis-inducing ligand induces neuronal death in a murine model of HIV central nervous system infection. Proc. Natl. Acad. Sci. USA **100**:2777–2782.
24. **Miura, Y., N. Misawa, N. Maeda, Y. Inagaki, Y. Tanaka, M. Ito, N. Kayagaki, N. Yamamoto, H. Yagita, H. Mizusawa, and Y. Koyanagi.** 2001. Critical contribution of tumor necrosis factor-related apoptosis-inducing ligand (TRAIL) to apoptosis of human CD4+ T cells in HIV-1-infected hu-PBL-NOD-SCID mice. J. Exp. Med. **193**:651–660.
25. **Mosier, D. E., R. J. Gulizia, S. M. Baird, D. B. Wilson, D. H. Spector, and S. A. Spector.** 1991. Human immunodeficiency virus infection of human-PBL-SCID mice. Science **251**:791–794.
26. **Pan, G., J. Ni, Y. F. Wei, G. Yu, R. Gentz, and V. M. Dixit.** 1997. An antagonist decoy receptor and a death domain-containing receptor for TRAIL. Science **277**:815–818.
27. **Pan, G., K. O'Rourke, A. M. Chinnaiyan, R. Gentz, R. Ebner, J. Ni, and V. M. Dixit.** 1997. The receptor for the cytotoxic ligand TRAIL. Science **276**:111–113.
28. **Ratain, M., and W. Plunkett.** 1997. Pharmacology, p. 875–889. *In* J. Holland, R. Bast, Jr., D. Morton, E. Frei, D. KuFe, and R. Weichselbaum (ed.), Cancer medicine, 4th ed. Williams and Wilkins, Baltimore, Md.
29. **Ruxrungtham, K., E. Boone, H. Ford, Jr., J. S. Driscoll, R. T. Davey, Jr., and H. C. Lane.** 1996. Potent activity of 2′-β-fluoro-2′,3′-dideoxyadenosine against human immunodeficiency virus type 1 infection in hu-PBL-SCID mice. Antimicrob. Agents Chemother. **40**:2369–2374.
30. **Strizki, J. M., S. Xu, N. E. Wagner, L. Wojcik, J. Liu, Y. Hou, M. Endres, A. Palani, S. Shapiro, J. W. Clader, W. J. Greenlee, J. R. Tagat, S. McCombie, K. Cox, A. B. Fawzi, C. C. Chou, C. Pugliese-Sivo, L. Davies, M. E. Moreno, D. D. Ho, A. Trkola, C. A. Stoddart, J. P. Moore, G. R. Reyes, and B. M. Baroudy.** 2001. SCH-C (SCH 351125), an orally bioavailable, small molecule antagonist of the chemokine receptor CCR5, is a potent inhibitor of HIV-1 infection in vitro and in vivo. Proc. Natl. Acad. Sci. USA **98**:12718–12723.
31. **Walker, U. A., B. Setzer, and N. Venhoff.** 2002. Increased long-term mitochondrial toxicity in combinations of nucleoside analogue reverse-transcriptase inhibitors. AIDS **16**:2165–2173.
32. **Westervelt, P., H. E. Gendelman, and L. Ratner.** 1991. Identification of a determinant within the human immunodeficiency virus 1 surface envelope glycoprotein critical for productive infection of primary monocytes. Proc. Natl. Acad. Sci. USA **88**:3097–3101.
33. **Yahata, T., K. Ando, Y. Nakamura, Y. Ueyama, K. Shimamura, N. Tamaoki, S. Kato, and T. Hotta.** 2002. Functional human T lymphocyte development from cord blood CD34+ cells in nonobese diabetic/Shi-scid, IL-2 receptor gamma null mice. J. Immunol. **169**:204–209.
34. **Yoshida, A., R. Tanaka, T. Murakami, Y. Takahashi, Y. Koyanagi, M. Nakamura, M. Ito, N. Yamamoto, and Y. Tanaka.** 2003. Induction of protective immune responses against R5 human immunodeficiency virus type 1 (HIV-1) infection in hu-PBL-SCID mice by intrasplenic immunization with HIV-1-pulsed dendritic cells: possible involvement of a novel factor of human CD4(+) T-cell origin. J. Virol. **77**:8719–8728.
35. **Yoshimura, K., R. Kato, K. Yusa, M. F. Kavlick, V. Maroun, A. Nguyen, T. Mimoto, T. Ueno, M. Shintani, J. Falloon, H. Masur, H. Hayashi, J. Erickson, and H. Mitsuya.** 1999. JE-2147: a dipeptide protease inhibitor (PI) that potently inhibits multi-PI-resistant HIV-1. Proc. Natl. Acad. Sci. USA **96**: 8675–8680.

Rev. Med. Virol. 2005; **15**: 169–178.
Published online 11 March 2005 in Wiley InterScience (www.interscience.wiley.com).
Reviews in Medical Virology
DOI: 10.1002/rmv.462

REVIEW

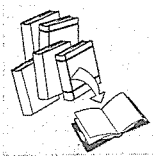

Death ligand-mediated apoptosis in HIV infection

Yoshiharu Miura* and Yoshio Koyanagi

Laboratory of Viral Pathogenesis, Research Center for AIDS, Institute for Virus Research, Kyoto University, Japan

SUMMARY

Apoptosis has been suggested to cause severe $CD4^+$ T cell depletion in patients infected with HIV. This review focuses on the biological events involved in death ligand-induced apoptosis during HIV infection. Among these ligands, TRAIL appears critical in HIV-infection. Death ligand-induced apoptosis might be a major pathogenic event in many virus-induced diseases including AIDS and the clarification of its mechanism will aid in the development of therapeutic strategies. Copyright © 2005 John Wiley & Sons, Ltd.

Received: 12 November 2004; Accepted: 15 November 2004

INTRODUCTION

Severe CD4 depletion is a hallmark of acquired immunodeficiency syndrome (AIDS) and the gradual loss of $CD4^+$ T cells leading to the onset of AIDS appears to be a result of infection with human immunodeficiency virus (HIV). Apoptosis, which has been shown to be significantly induced in HIV-infected individuals, seems to trigger the CD4 depletion during disease progression. Two major pathways have been identified from extensive molecular biology-based analysis; an extrinsic pathway, which is initiated by the binding of tumor-necrosis factor (TNF) family ligands to their cognate death receptors, and an intrinsic pathway, which is initiated by an internal sensor system that mainly transmits signals to the mitochondria and is mediated by Bcl-2-related proteins [1,2]. This review summarises our present level of understanding of the molecular mechanisms behind the extrinsic pathway of T lymphocyte apoptosis with HIV infection.

Corresponding author: Dr Y. Miura, Institute for Virus Research, Kyoto University, 53 Shougoin-kawaramachi, Sakyou-ku, Kyoto 606-8507, Japan. E-mail: ymiura@virus.kyoto-u.ac.jp

Abbreviations used

AICD, activation-induced cell death; AIDS, acquired immunodeficiency syndrome; cFLIP, cellular FLICE inhibitory protein; DISC, death-inducing signaling complex; FADD, Fas-associated death domain; FLICE, FADD-like ICE; HIV, human immunodeficiency virus; TNF, tumor necrosis factor; TRAIL, TNF-related apoptosis-inducing ligand.

HIV INFECTION AND APOPTOSIS

Apoptosis is thought to occur in HIV-infected individuals and arise from the following mechanisms; HIV-induced syncytium formation, HIV protein-induced cell death, activation-induced cell death (AICD) and bystander cell killing (Figure 1). Ballooning cells and multinucleic giant cells are frequently found in virus-infected cell cultures *in vitro*. The cytopathic effect (CPE) in HIV-infected $CD4^+$ T cell cultures is known to be the formation of syncytia between productively infected and adjacent uninfected cells and clearly induces the apoptosis in these cells, obviously dependent on viral replication [3,4]. Syncytia are also found in infected tissues [5,6]. The envelope glycoprotein complex of gp120-gp41 on the surface of the infected cells, which causes the death of both infected and adjacent uninfected cells, seems to be one of the dominant apoptosis-inducing molecules encoded by the HIV-1 genome (Figure 2). The envelope expressed on the plasma membrane of infected cells can interact with the CD4 molecule and a suitable co-receptor to trigger cell-to-cell fusion; resulting in syncytia and subsequently apoptosis [7,8]. It was reported that mitochondria-dependent apoptosis (intrinsic pathway) occurs with the fusion of envelope-expressing cells with CD4- and coreceptor-expressing target cells [9]. The shedding of HIV-encoded proteins such as envelope, Tat and Vpr (Figure 2) has also been shown to trigger apoptosis in both infected and

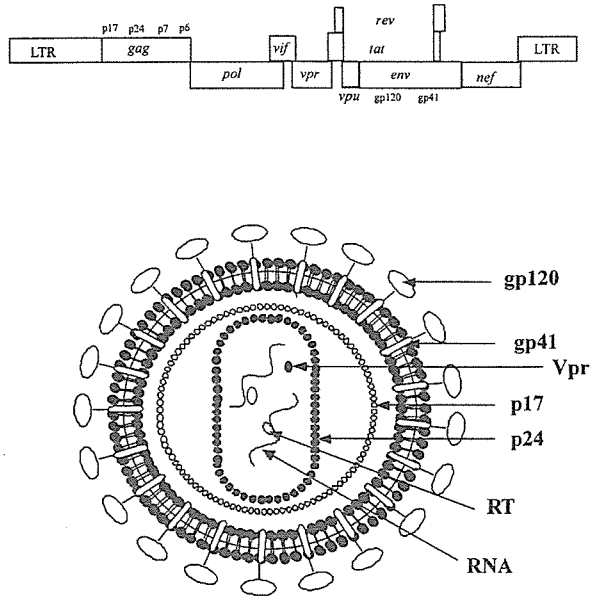

Figure 1. The HIV-1 provirus and its proteins. Gag and Gag-Pol polyprotein precursors are processed by the viral protease into nine subunits: protease, reverse transcriptase, integrase, matrix, capsid, p2, nucleocapsid, p1 and p6. Env is cleaved by cellular proteases, such as furin, into surface gp120 and transmembrane gp41 moieties. Tat is a transcriptional and translational regulator of expression. The RNA target region, the transactivation response (TAR) element, is located at the 5′ end of all viral transcripts. Rev has a major role in the nuclear-export of large HIV-1 RNA (gag and env transcripts) and regulates the shift between early and late viral gene expression. The viral-infectivity factor (Vif), viral protein u (Vpu), viral protein R (Vpr) and negative effector (Nef) proteins are known as accessory proteins because they are dispensable for viral growth in some cell-culture systems

uninfected cells in culture. Tat effectively induces apoptosis by downregulating the expression of Bcl-2 and upregulating the expression of Bax as well as caspase 8 [10,11]. On the other hand, the typical intrinsic pathway can be triggered by the soluble form of Vpr protein, which causes a rapid disintegration of the mitochondrial transmembrane potential in intact cells, as well as the release of cytochrome c and subsequent apoptosis [12]. On the other hand, AICD, which is known to be dependent on death receptors, was observed in *ex vivo* cultured T cells from HIV-infected patients following activation with mitogens, superantigens or antibodies specific for TCR [13]. AICD was originally found to occur during the elimination of prolongly activated T cells when the inflammatory reaction is coming to an end. Significantly, increased destruction of $CD4^+$ T cells in secondary lymphoid organs such as lymph nodes and spleen has been reported in HIV-infected individuals [14]. In addition, it has been postulated that HIV-1 infection causes uninfected $CD4^+$ T cells to die, and a bystander cell killing mechanism has been suggested based on histopathological analyses of lymph nodes in HIV-1-infected individuals and simian immunodeficiency virus (SIV)-infected monkeys [15]. The persistent existence of HIV proteins (Tat, gp120, Nef, Vpu) *in vivo* might stimulate apoptosis in uninfected bystander cells.

APOPTOSIS AND DEATH LIGAND

The extrinsic pathway arises from the binding of the ligand molecule to its respective membrane-bound death receptor and the engagement of the caspase cascade (Figure 3). Death receptors are members of the TNF receptor superfamily, which initiate a rapid activation of the caspase cascade and commit the cell to apoptosis when triggered by their cognate TNF family ligands. These ligands include Fas ligand (FasL), TNF, TNF-related apoptosis-inducing ligand (TRAIL) and TWEAK, and all of the death receptors possess both a cysteine-rich extracellular domain and an intracellular cytoplasmic sequence motif, known as the death domain (DD).

FasL is a type 2 membrane protein and an exclusive ligand for Fas, inducing Fas-mediated apoptosis [16]. The ligation of FasL to Fas triggers the Fas monomers to combine into trimeric Fas-complexes (Figure 3). The intracellular domain of Fas contains the DD, a stretch of 80 amino acids. After the trimerisation of Fas molecules, the DD recruits many cytosol proteins and forms a multi-protein death-inducing signaling complex (DISC) [17,18]. Immediately following Fas/FasL ligation, the prompt recruitment of a serine-phosphorylated adaptor molecule, Fas-associated DD (FADD), is induced and then the Fas/FADD interaction is coordinated through the highly conserved DD motifs found in both proteins. FADD serves as a bridge between Fas and downstream molecules, such as Fas-like IL-1β converting enzyme (FLICE) as well as cytotoxicity-dependent APO-1-associated protein 3 (CAP3). The FADD-FLICE/CAP3 interaction allows the liberation of caspase 8 and CAP3 in an active form from their dormant states. Formation of the DISC, which is composed of Fas, FADD and FLICE/CAP3, results in the initiation of a signal cascade to downstream target molecules, such as procaspase 3, 6 and 7. The activated